

**A novel and highly innovative method for
visualization and characterization of the
insect surface inward barriers**

Dissertation

der Mathematisch-Naturwissenschaftlichen Fakultät
der Eberhard Karls Universität Tübingen
zur Erlangung des Grades eines
Doktors der Naturwissenschaften
(Dr. rer. nat.)

vorgelegt von
Yiwen Wang (M.Sc.)
aus Tianjin (China)

Tübingen
2018

Tag der mündlichen Prüfung: 14.11.2018

Dekan: Prof. Dr. Wolfgang Rosenstiel

1. Berichterstatter: PD Dr. Bernard Moussian
2. Berichterstatter: Prof. Dr. Matthias Schwab

I dedicate this thesis to my parents, Jianqun and Yan,
and to my wife and son, Ting and Yunhuai.

Table of Contents

Abbreviations	1
Abstract	2
Zusammenfassung	4
1. Publications	6
2. Contribution to the Publication	7
3. Introduction	8
4. Results.....	11
4.1. The Eosin Y based method for in situ analysis of cuticle barrier	11
4.2. Double cuticle barrier in whitefly and bedbug.....	13
4.3. Eosin Y method using in genetic level research	14
5. Discussion.....	16
5.1. Eosin Y penetration is blocked by cuticular hydrocarbons (CHC).....	16
5.2. The Eosin Y method reveals the regionalized distribution of CHC on the insect surface.	17
5.3. Outlook.....	18
5.3.1. The agricultural application of Eosin penetration assay	18
5.3.2. The application of Eosin penetration assay in genetic study on cuticle lipid layer formation.....	19
6. References	22
Appendix 1: Regionalization of surface lipids in insects.....	25
Appendix 2: Double cuticle barrier in two global pests, the whitefly <i>Trialeurodes vaporariorum</i> and the bedbug <i>Cimex lectularius</i>	34
Appendix 3: The ABC transporter Snu and the extracellular protein Snsl cooperate in the formation of the lipid-based inward and outward barrier in the skin of <i>Drosophila</i>	39
Acknowledgement - Danksagung.....	52

CURRICULUM VITAE	53
Disclosures-Erklärungen:	57

Abbreviations

ABCH-9C	ATP-binding cassette transporter family H member 9C
ABC transporter	ATP-binding cassette transporter
CHC	Cuticular hydrocarbons
DDT	Dichlorodiphenyltrichloroethane
ECM	Extracellular matrix
FTIR	Fourier-transform infrared spectroscopy
hpRNA	Hairpin Ribonucleic acid
snsI	Snustorr snarli (CG2837)
snu	Snustorr (CG9990)
T_c	Critical temperature
T_m	Melting temperature
T_{pe}	Temperature of penetration of Eosin Y

Abstract

In insects, cuticular hydrocarbons (CHCs) play a critical role in the establishment of the barrier that prevents both dehydration and penetration of environmental hazards such as pathogens and toxic molecules. While rich data is available on CHC composition in different species and their relationship with insect dehydration resistance or susceptibility, we know little about their distribution, organization and their functional roles in the formation of the insect surface inward barrier. Here, I present my work on the development of an Eosin Y penetration method to visualize and characterize the insect surface inward barrier. In the Eosin Y penetration method, the investigated insect is incubated in Eosin Y solution at certain temperatures. The dye penetrates different regions of the insect cuticle at distinct temperatures. The temperatures, at which the Eosin Y penetrated the certain cuticle region and stained the tissue, is recorded as the “temperature of penetration of Eosin Y” T_{p_e} of the respective region. Differences between T_{p_e} values indicate differences in lipid composition in these regions.

This Eosin Y penetration method is easy, quick, cost limited and can be commonly used in different insect species. We have used this method to analyse the barrier distribution in fruit fly (*Drosophila melanogaster*) adults and larvae, locust (*Locusta migratoria*) nymphs, mealworm (*Tenebrio molitor*) larvae, whitefly (*Trialeurodes vaporariorum*) adults and bedbug (*Cimex lectularius*) nymphs. The results indicate that the distribution of surface lipids in most insects is regionalized. Furthermore, in some species, such as whitefly and bedbug, two barriers exist in parallel in same regions of the cuticle with

presumably distinct temperature-sensitive and lipid-based physico-chemical material properties.

We also applied this method to determine the role of certain enzymes such as the ABCH-9C transporter *Snu* and the cuticle protein *Sns1* in the establishment of the cuticular inward barrier.

I show that this new method gives us new insights into the theme cuticle permeability, and I believe that it can be widely used in designing new insecticides, which are more efficiently taken up by specific target pest species. Additionally, the Tp_e alteration is an excellent readout for genetic screens to study the molecular pathways of cuticle inward barrier formation i.e. of the establishment of the CHC layer.

Zusammenfassung

Bei Insekten spielen Kohlenwasserstoffe in der Kutikula (engl. cuticular hydrocarbons, CHC) eine entscheidende Rolle bei der Herstellung der wasserdichten Barriere, die sowohl die Dehydratation als auch das Eindringen von Umweltgefahren wie Krankheitserregern und potentiell toxischen Molekülen verhindert. Während umfangreiche Daten über die CHC-Zusammensetzung bei verschiedenen Arten und ihre Beziehung zur Insekten-Dehydratationsresistenz verfügbar sind, wissen wir wenig über ihre Verteilung, Organisation und ihre funktionellen Rollen bei der Bildung der Einwärtsbarriere der Insektenoberflächen. Hier präsentiere ich meine Arbeiten zur Entwicklung einer Eosin-Y-Penetrationsmethode zur Visualisierung und Charakterisierung der Einwärts-Barriere der Insektenoberfläche. Bei der Eosin-Y-Penetrationsmethode wird das Insekt in Eosin Y-Lösung bei bestimmten Temperaturen inkubiert. Der Farbstoff dringt bei unterschiedlichen Temperaturen in verschiedene Bereiche der Insektenhaut ein. Die Temperaturen, bei denen das Eosin Y eine bestimmte Hautregion durchdrang und das Gewebe unter solchen Regionen färbte, können als „Temperatur der Penetration von Eosin Y“ T_{pe} einer solchen Region aufgezeichnet werden. Unterschiede zwischen den T_{pe} -Werten zeigen Unterschiede in der Lipidzusammensetzung in den jeweiligen Regionen an.

Diese Eosin Y-Penetrationsmethode ist einfach, schnell, kostengünstig und kann bei verschiedenen Insektenarten verwendet werden. Wir haben diese Methode bereits verwendet, um die Barriereverteilung in Adulten und Larven der Fruchtfliege (*Drosophila melanogaster*), Nymphen der Wander-Heuschrecke (*Locusta migratoria*),

Larven von Mehlwürmern (*Tenebrio molitor*), Adulten der Weißen Fliege (*Trialeurodes vaporariorum*) und Wanzen-Nymphen (*Cimex lectularius*) zu analysieren. Die Ergebnisse legen nahe, dass die Verteilung von Oberflächenlipiden der meisten Insekten regionalisiert ist. Darüber hinaus existieren bei einigen Arten, wie der Weißen Fliege und der Wanze, zwei Barrieren, die augenscheinlich in den gleichen Regionen der Kutikula unterschiedliche temperaturempfindliche und lipid-basierte physikalisch-chemische Materialeigenschaften aufzeigen.

Ich habe diese Methode auch angewendet, um die Rolle bestimmter Enzyme wie des ABCH-9C-Transporters *Snu* oder des Kutikulaproteins *Snsl* bei der Bildung der kutikulären Einwärts-Barriere zu bestimmen.

Diese neue Methode verschafft neue Einblicke in die Permeabilität der Kutikula, und es ist davon auszugehen, dass sie in großem Umfang bei der Entwicklung neuer Insektizide verwendet werden kann, damit diese von bestimmten Schädlingen effizienter aufgenommen werden können. Zusätzlich können T_p -Veränderungen auch bei Genom-Screens verwendet werden, um molekulare Prinzipien der Bildung von Kutikula-Kohlenwasserstoffschichten zu untersuchen und beteiligte Gene zu identifizieren.

1. Publications

1. Wang, Yiwen; Yu, Zhitao; Zhang, Jianzhen; Moussian, Bernard (2016): **Regionalization of surface lipids in insects.** In: *Proceedings. Biological sciences* 283 (1830). DOI: 10.1098/rspb.2015.2994.
2. Wang, Yiwen; Carballo, Rocio Gallego; Moussian, Bernard (2017): **Double cuticle barrier in two global pests, the whitefly *Trialeurodes vaporariorum* and the bedbug *Cimex lectularius*.** In: *The Journal of experimental biology* 220 (Pt 8), S. 1396–1399. DOI: 10.1242/jeb.156679.
3. Zuber, Renata; Norum, Michaela; Wang, Yiwen; Oehl, Kathrin; Gehring, Nicole; Accardi, Davide; Bartozsewski, Slawomir; Berger, Jürgen; Flotenmeyer, Matthias and Moussian, Bernard (2018). **The ABC transporter Snu and the extracellular protein Sns1 cooperate in the formation of the lipid-based inward and outward barrier in the skin of *Drosophila*.** In: *Eur J Cell Biol.* 97(2), S. 90-101. DOI: 10.1016/j.ejcb.2017.12.003.

2. Contribution to the Publication

Publication 1: **Regionalization of surface lipids in insects (Proceedings of the Royal Society: B)**

Contribution: I designed and performed the Eosin Y penetration tests on fruit flies and mealworms. Thereby, I discovered the regionalization of insect cuticle lipids and defined the term Tp_e and drew the Tp_e maps to the fruit fly and the mealworm.

Publication 2: **Double cuticle barrier in two global pests, the whitefly *Trialeurodes vaporariorum* and the bedbug *Cimex lectularius* (The Journal of Experimental Biology)**

Contribution: I performed the penetration assays on white flies and bedbugs with Eosin Y and two other dyes and discovered the existence of the double cuticle barrier in white flies and bedbugs.

Publication 3: **The ABC transporter *Snu* and the extracellular protein *Sns1* cooperate in the formation of the lipid-based inward and outward barrier in the skin of *Drosophila*. (European Journal of Cell Biology)**

Contribution: I designed and performed the embryonic Eosin Y penetration assay and discovered that *snu* and *sns1* are needed for inward cuticle barrier construction.

3. Introduction

Insects are the largest class within the arthropod phylum. They occupy almost every terrestrial niche, but are quasi absent from aquatic habitats. The successful radiation relies mainly on their extracellular coat, the so-called cuticle, which covers the whole body. The insect cuticle serves as an exoskeleton for locomotion, protects the insect body against mechanical damage, and acts as an impermeable barrier, providing protection against dehydration and invasion of environmental hazards such as pathogens and toxic molecules.

The insect cuticle is a stratified extracellular matrix (ECM), which is formed at the apical side of the monolayer of epidermal cells. It can generally be divided into three horizontal layers (Moussian 2010): The procuticle is the inner chitin-protein matrix adjacent to the apical surface of the epidermis. It is overlain by the protein-network, named epicuticle. The outermost layer is the envelope, which remains poorly characterized. The envelope is covered by a matrix of cuticular hydrocarbons (CHCs). This hydrophobic layer is commonly believed to play a critical role in the establishment of the barrier in both outward and inward directions (Gibbs 2002, Blomquist GJ 2010).

An insect may have more than 100 different CHCs, which consist mainly of three types of molecules: alkanes, methyl-alkanes and waxes (Blomquist, Nelson et al. 1987, Lockey 1988, Gibbs 1998). Their composition varies between species, stages and gender (Gibbs and Crowe 1991).

CHCs have been repeatedly shown to play a crucial role in the function of the outward barrier, in other words, the barrier against dehydration. In the middle of the last century, a phenomenon was commonly observed, that the rates of water loss from insect bodies remain constant and very low as the temperature is raised to moderate ranges, but increase dramatically when the temperature reaches or oversteps a critical temperature (T_c) (Ramsey 1935, Wigglesworth 1945). The T_c values vary between species (Gibbs 2002). A comprehensible explanation of this phenomenon is represented in the lipid melting model: the sudden breakdown of cuticular permeability to water at a certain temperature relies on the transition of CHCs from an impermeable solid state to a permeable fluid state (lipid melting) at this temperature (Ramsey 1935, Gibbs 1998). This hypothesis is supported by the observation that in most species the critical temperatures of cuticular permeability (T_c) were similar to temperatures, which cause CHC melting. The consistency between T_c and T_m was also observed in individual grasshoppers (Rourke and Gibbs 1999). Although the lipid-melting model has achieved common acceptance, numerous limitations still exist.

First, to determine the T_c and T_m values, special technics and expensive instruments are required. Only a limited number of insect species have been examined to date (Gibbs 2002).

Second, not for all examined species the obtained data are in agreement with the lipid-melting model. For example, the mealworm (*Tenebrio molitor*) larvae have a T_m higher than 80°C. It is far distinct from its T_c value, which is between 50°C and 60°C (Wigglesworth 1945, Gibbs and Crowe 1991).

Third, the T_c/T_m analysis can only be conducted efficiently with large insects, such as grasshoppers and crickets (Gibbs and Crowe 1991, Rourke and Gibbs 1999, Young, Larabee et al. 2000). For many insects with small body size, such as the fruit fly, determination of T_c/T_m is rather difficult, or even impossible, especially when individual information is needed.

Fourth, different regions of the insect surface have different CHC composition (Gibbs and Crowe 1991). But the T_c is an index of the whole body. The analysis of the T_m value of a single body part of an insect is obviously limited by the body size.

Finally, for the measurement of T_m , surface lipids have to be dissolved and separated from the cuticle, which may alter the original construction or organisation of the lipids mix.

In my works, I designed a new *in situ* method to analyse the barrier function of the CHC layer with dependence of the temperature. Instead of monitoring water loss at different temperatures, we study the ability of the insect to take up a dye, such as Eosin Y in order to reflect cuticle barrier function at the tissue level. Compared to traditional methods, the new method is quicker, cheaper, generally without body size limitation and, most importantly, can distinguish the barrier function between different regions of the surface of one insect.

4. Results

4.1. The Eosin Y based method for in situ analysis of cuticle barrier

To visualize cuticle permeability, I developed a new analysis system based on dye penetration. Eosin Y, a harmless food dye with a bright red colour, was used for this purpose. The analysis was easily performed by immersing the investigated insect in the dye solution at certain temperatures. Dye penetrates certain cuticle region when the CHC barrier at this region is broken down at this temperature.

The fruit fly (*Drosophila melanogaster*) was first used to establish this method. Indeed, I found that the inert Eosin Y penetrates different regions of the adult body at distinct temperatures. At room temperature (25 °C), most parts of the insect surface were impermeable to Eosin Y. Only two sensory organs on the head, the antennal and maxillary palps, were stained by Eosin Y. These organs became also impermeable to Eosin Y at 4 °C. Eosin staining of the fly body was unchanged at 30 °C and 37 °C. At 40 °C, mouthparts became red. The whole head became permeable at 55 °C.

The wing is also a very special organ, which is a cell free structure built by two cuticle layers only. The wing was impermeable to Eosin Y until 45 °C. At 50 °C, the dye clearly penetrated first the lower edge of the wing and the upper edge at 55 °C or 58 °C.

The legs were also not uniformly stained. The joints and the claw were stained at 50 °C, and the legs were completely stained at 58 °C.

Moreover, I showed that the cuticle permeability to Eosin Y depends on the phase transition of the surface lipid layer. First, I demonstrated that the heat-induced permeability of the cuticle is reversible. When after incubation at 58 °C, I cooled down the fly body, the cuticle became impermeable again. I call this experiment an annealing assay. This result indicates that induction of permeability does not stem from damages by heating, but rather from a transition of a matrix between different states. Second, I tested whether lipid solvents are able to wash away this barrier. Chloroform, hexane and heptane are common solvents used for extracting insect surface lipids. Flies treated with these solvents became systematically permeable to Eosin Y after short incubation at room temperature. This result indicates that the barrier consists of hydrophobic compounds like lipids and waxes.

Next, I analyzed Eosin Y penetration into the cuticle of mealworm (*Tenebrio molitor*) larvae and locust (*Locusta migratoria*) nymphs. Eosin Y penetration in the mealworm and locust cuticle is also temperature-dependent. Furthermore, the Eosin Y penetration is regionalized in the mealworm larvae, whereas it is not in locust nymphs. It is interesting that the tergites, the main cuticle part of mealworm larvae, became permeable at 90 °C, which corresponds to the recorded T_m value (> 80 °C) for mealworm larvae (Wigglesworth 1945). Moreover, the spiracles, the openings of the tracheal system needed for gas exchange, became stainable at 60 °C (Wigglesworth 1945), which corresponds to the determined T_c value. Together, I suggest that this property of the

spiracle cuticle is the reason why mealworms lose water when the temperature rises above 60 °C, far lower than the T_m value of the whole body.

4.2. Double cuticle barrier in whitefly and bedbug

The greenhouse whitefly (*Trialeurodes vaporariorum*) is a major pest of greenhouse crops and vegetables. The bedbug (*Cimex lectularius*) is a famous parasitic insect. I studied cuticle barrier permeability in these two global pests. Similar to the situations in fruit flies and mealworms, Eosin Y penetrated the whitefly and bedbug cuticle in a temperature-dependent and regionalized manner. Additionally, I found, in contrast to the single barrier in fruit flies, that there are two barriers with different temperature-sensitive and lipid-based physico-chemical material properties acting in parallel to protect these insects against penetration of hydrophilic molecules.

The whitefly wing cuticle was impermeable to Eosin Y at 25 to 60 °C. Penetration of the dye started at 70 °C first at the margin and the single wing vein. The entire wing surface was stained first at 80 °C. Incubation of the cuticle with chloroform only rendered the wing margin and wing vein, but not the surface, penetrable to Eosin Y. I additionally combined the effects of temperature and chloroform washing. I found that the entire wing surface became permeable at 60 °C after incubation in chloroform. The intensity was the same as at 80 °C with or without chloroform washing. This result indicates that there are at least two different barriers: one is barrier A, which is damageable by lipid solvents, while the other is barrier B, which is more sensitive to temperature. Furthermore, after the annealing assay, I found that the barrier A is irreversible, when it is broken down by

heating at 80 °C, while barrier B breakdown is still reversible. Altogether, I suggest, that barrier A consists of free compounds, which adhere on the surface, while the barrier B consists of compounds, which are anchored on the cuticle. The additive effect of chloroform and temperature on Eosin Y penetration was also observed in the bedbug cuticle.

Additionally, I tested two new dyes, Bromophenol blue and methylene blue in penetration assays. These two dyes behave identically to Eosin Y. This result indicates that the properties of cuticle barriers, which I recorded through penetration assays, are independent from the applied dye.

4.3. Eosin Y method using in genetic level research

The Eosin Y based penetration assay provides a quick and easy method to visualize the alteration of barrier function based on genetic differences.

Years ago, our group conducted a screen for cuticle defective phenotypes caused by RNAi-driven knockdown of late embryonic epidermal expressed genes to identify new factors of cuticle formation. Two genes *CG9990* and *CG2837* attracted our attention. Knockdown of *CG9990* expression caused lethality at the end of embryonic development. *CG2837* knockdown larvae died quickly after hatching. Both *CG9990* and *CG2837* knock-downed larvae dehydrate rapidly. We named *CG9990* *snustorr* (*snu*, Swedish for bone-dry) and *CG2837* *snustorr snarlik* (*snsI*, Swedish for *snu*-like).

To explore whether the cuticle of *snu* and *sns1* knockdown larvae is more permeable than the wild-type cuticle, we immersed these larvae in Eosin Y. Wild-type larvae remain unstained after incubation in Eosin Y at room temperature and at 40 °C. They take up Eosin Y at 55 °C. Reduction of *Snu* and *Sns1* function causes a dramatic uptake of Eosin Y through the integument at 25 °C or 40 °C, respectively. Applying this protocol, we also tested the permeability of the wing cuticle in wild-type flies and flies expressing hpRNA against *snu* or *sns1* transcripts in the wing. Wild-type wings do not take up Eosin Y at 25 °C. At 50 °C, by contrast, two areas in the posterior edge of the wings become red. Wings with reduced *snu* activity are impermeable to Eosin Y at 25 °C, whereas the entire wing blades are stained by Eosin Y at 50 °C. Reduction of *sns1* expression in wings does not interfere with Eosin Y uptake. Together, these findings demonstrate that *snu* and *sns1* are needed for inward cuticle barrier construction.

Further studies showed that *snu* encoded an ABC transporter, which localises in the apical plasma membrane of epidermal cells, and *sns1* encodes a secreted protein, which localises to the tips of pore canals within the cuticle. Under transmission electron microscopy, we found both *snu* and *sns1* deleted larvae had an impaired envelope (the outermost cuticle layer).

5. Discussion

5.1. Eosin Y penetration is blocked by cuticular hydrocarbons (CHC).

Just like the widely accepted lipid-melting model, we suggest that the temperature dependent alteration of the dye permeability of the insect surface is caused to a considerable extent by the melting of a cuticular lipid layer.

Three evidences support this interpretation:

First, the dye impermeable barriers are completely or partially broken down through organic solvents. After short incubation in chloroform, a solvent commonly used to extract surface lipids in insects, Eosin Y penetrates the entire adult cuticle of the fruit flies and the locust nymph already at 25 °C. Chloroform treatment also breaks the surface barrier of whiteflies and bedbugs in certain regions. Furthermore, the penetration temperatures of other regions become much lower after chloroform treatment.

Second, our T_{p_e} results are generally consistent with previous reports on T_m and T_c in different insect species. The T_{p_e} of the mealworm larval tergite, the major part of their surface, is between 80 °C – 90 °C. This result corresponds to reports that mealworm larvae have a high T_m value of above 80 °C (Wigglesworth 1945). The surface of locust nymphs is slightly stained at 48 °C. This is very close to the T_c value of 47 °C determined for the adult locust (Loveridge 1968). According to the lipid-melting model, T_m values should be close to the T_c values.

Third, the alteration of T_{p_e} through genetic manipulation correlates with envelope integrity and the waterproof function of the cuticle in the fruit fly. Knockdown of transcripts coding for the ABCH-9C transporter Snu or the extracellular protein Sns1 in fruit fly embryos causes defects in the envelope and uncontrolled dehydration. The T_{p_e} of the respective embryos/larvae shifts from 55 °C to 25 °C and 40 °C, respectively. We have cooperated with a Chinese group to analyse the function of the putative orthologue of Snu in locusts, and confirmed that the ABCH-9C transporters have conserved function in establishing the inward barrier in fruit flies and locusts (Yu, Wang et al. 2017).

5.2. The Eosin Y method reveals the regionalized distribution of CHC on the insect surface.

Different regions of the fruit fly surface become permeable to Eosin Y at different temperatures. Likewise, Eosin Y penetrates different parts of the cuticle of mealworm larvae, whitefly wings and bedbugs at distinct temperatures. These findings indicate that different regions of the insect surface are composed of specific structural and chemical factors including CHCs. This conclusion is supported by FTIR spectroscopy data indicating that the melting temperatures of CHCs of different body parts of the grasshopper (*Melanoplus sanguinipes*) are different from each other (Gibbs and Crowe 1991).

No regionalization was observed on the surface of locust first-instar nymphs. This is maybe because the freshly hatched and unpigmented nymphs have not yet developed a

mature and regionalized lipid layer. This possibility should be tested by staining of older animals.

Nevertheless, our data suggest that most if not all insects have regionalized surface lipid composition. Conceivably, regionalization suggests the existence of region-specific genetic mechanisms for CHCs production and localization during cuticle formation and renewal. Thanks to the well-developed genetic tools, the fruit fly is the perfect model insect to study the genetic programme of barrier regionalization.

5.3. Outlook

5.3.1. The agricultural application of Eosin penetration assay

Contact insecticides are the major group of insecticides, which include very famous products, such as DDT, cypermethrin, sumithion, dieldrin and carbaryl (Moriarty and French 1971, Theisen, Miller et al. 1991, Juarez 1994, Lin, Jin et al. 2012). The uptake of insecticides seems to be specific to body regions. For example, dieldrin is more effectively taken up by the pronotum of cockroaches (*Periplaneta americana*) rather than by their wings (Moriarty and French 1971). The pulvilli of tsetse flies (*Glossina spp.*) have been reported to be very effective in DDT and pyrethrum uptake (Potts and Vanderplank 1945). Our Eosin Y method has the potential to draw maps of lipid sub-regions of the surface of any insect of interest (Tp_e maps). These Tp_e maps will expand our knowledge, which can be used to find out the preferred penetration site and to

optimize the mode of action of contact insecticides. Furthermore, species-specific insecticides may be designed according to the distinct Tp_e in different species.

5.3.2. The application of Eosin penetration assay in genetic study on cuticle lipid layer formation

The use of the fruit fly as a model organism for genetic research started over 100 years ago (Ugur, Chen et al. 2016). Many landmark genetic discoveries were developed in this insect. Numerous powerful genetic tools have been developed for fruit fly research, which ensure the fruit fly as the most popular model animal in genetic research.

Large-scale approaches led to the identification and characterization of several genes that are involved in lipid biosynthesis and essential for CHC production and biology (Dembeck, Boroczky et al. 2015, Chiang, Tan et al. 2016), In general, as expected, the CHC profile in adult flies depends on the activity of enzymes of the lipid biosynthesis pathway. In one study 12 genes were found to be essential (Chiang, Tan et al. 2016), in another study 24 genes (Dembeck, Boroczky et al. 2015). There are also many single genes, which code for enzymes involved in general lipid biosynthesis such as acetyl-CoA-carboxylase (*acc*) (Parvy, Napal et al. 2012), methyl-branched CHC specific fatty acid synthase (FASN2) (Chung, Loehlin et al. 2014), desaturase-1 (*desat1*) (Wang, da Cruz et al. 2016) and aldehyde oxidative decarboxylase P450 (*cyp4g1*) (Qiu, Tittiger et al. 2012), that were reported to be required for cuticle waterproofness. By contrast, the

role of the CHCs as potential components of the cuticle inward barrier for xenobiotic molecules has been rarely investigated to date at the molecular level.

With our Eosin Y penetration method, we have already identified the ABCH-9C transporter (Snu) and the cuticular secreted protein (SnsI) as essential factors in the formation of the inward barrier. We plan to use this method to test for more candidate genes, which have been previously reported to be involved in the constitution of the outward barrier.

Interestingly, the formation of the cuticular inward barrier requires not only the genes relevant in lipid production or transport. We found that Knickkopf (Knk), a key factor of chitin organization (Moussian, Tang et al. 2006), is also needed for cuticle impermeability. The wings of flies with wing-specific down-regulated *knk* expression showed a lower Tp_e on the wings and loss of regionalization (Li, Zhang et al. 2017). After establishment of the procuticle (chitin layer), the newly produced CHC materials have to be transported through the channels called pore canals to the surface. We hypothesise that the function of pore canals relies on correct chitin organization in the procuticle, which depends on Knk. The effect of Knk on cuticle impermeability is hence probably indirect and due to reduced lipid transport through the defective pore canals.

Another interesting aspect is the yet unknown genetic mechanisms of the inhomogeneous distribution of the cuticle lipids. Our Eosin Y penetration method provides an easy, quick and cost-limited way to monitor the fine alteration on the composition and distribution of cuticle surface lipids. We plan to perform a new large-scale genomic screen for the

identification and characterization of the factors involved in formation and regionalization of the cuticle inward barrier.

All these data will help us to understand the process of formation of the functional cuticle inward barrier in insects and thereby identify new target genes for pest control.

6. References

- Blomquist GJ, B. A.-G. (2010). "Insect hydrocarbons: biology biochemistry and chemical ecology." Cambridge University Press.
- Blomquist, G. J., D. R. Nelson and M. Derenobales (1987). "Chemistry, Biochemistry, and Physiology of Insect Cuticular Lipids." *Archives of Insect Biochemistry and Physiology* 6(4): 227-265.
- Chiang, Y. N., K. J. Tan, H. Chung, O. Lavrynenko, A. Shevchenko and J. Y. Yew (2016). "Steroid Hormone Signaling Is Essential for Pheromone Production and Oenocyte Survival." *Plos Genetics* 12(6).
- Chung, H., D. W. Loehlin, H. D. Dufour, K. Vaccarro, J. G. Millar and S. B. Carroll (2014). "A Single Gene Affects Both Ecological Divergence and Mate Choice in *Drosophila*." *Science* 343(6175): 1148-1151.
- Dembeck, L. M., K. Boroczky, W. Huang, C. Schal, R. R. H. Anholt and T. F. C. Mackay (2015). "Genetic architecture of natural variation in cuticular hydrocarbon composition in *Drosophila melanogaster*." *Elife* 4.
- Gibbs, A. and J. H. Crowe (1991). "Intraindividual Variation in Cuticular Lipids Studied Using Fourier-Transform Infrared-Spectroscopy." *Journal of Insect Physiology* 37(10): 743-748.
- Gibbs, A. G. (1998). "Water-proofing properties of cuticular lipids." *American Zoologist* 38(3): 471-482.
- Gibbs, A. G. (2002). "Lipid melting and cuticular permeability: new insights into an old problem." *Journal of Insect Physiology* 48(4): 391-400.
- Juarez, P. (1994). "Inhibition of Cuticular Lipid-Synthesis and Its Effect on Insect Survival." *Archives of Insect Biochemistry and Physiology* 25(3): 177-191.

Li, K., X. Zhang, Y. Zuo, W. Liu, J. Zhang and B. Moussian (2017). “Timed Knickkopf function is essential for wing cuticle formation in *Drosophila melanogaster*.” *Insect Biochem Mol Biol* 89: 1-10.

Lin, Y. Y., T. Jin, L. Zeng and Y. Y. Lu (2012). “Cuticular penetration of beta-cypermethrin in insecticide-susceptible and resistant strains of *Bactrocera dorsalis*.” *Pesticide Biochemistry and Physiology* 103(3): 189-193.

Lockey, K. H. (1988). “Lipids of the Insect Cuticle – Origin, Composition and Function.” *Comparative Biochemistry and Physiology B-Biochemistry & Molecular Biology* 89(4): 595-645.

Loveridge, J. P. (1968). “Control of Water Loss in *Locusta Migratoria Migratorioides* R and F .2. Water Loss through Spiracles.” *Journal of Experimental Biology* 49(1): 15.

Moriarty, F. and M. C. French (1971). “The uptake of dieldrin from cuticular surface of *Periplaneta american L.*” *Pest Biochem Physiol* 1: 286-292.

Moussian, B. (2010). “Recent advances in understanding mechanisms of insect cuticle differentiation.” *Insect Biochemistry and Molecular Biology* 40(5): 363-375.

Moussian, B., E. Tang, A. Tønning, S. Helms, H. Schwarz, C. Nüsslein-Volhard and A. E. Uv (2006). “*Drosophila* Knickkopf and Retroactive are needed for epithelial tube growth and cuticle differentiation through their specific requirement for chitin filament organization.” *Development* 133(1): 163-171.

Parvy, J. P., L. Napal, T. Rubin, M. Poidevin, L. Perrin, C. Wicker-Thomas and J. Montagne (2012). “*Drosophila melanogaster* Acetyl-CoA-Carboxylase Sustains a Fatty Acid-Dependent Remote Signal to Waterproof the Respiratory System.” *Plos Genetics* 8(8).

Potts, W. and F. Vanderplank (1945). “Mode of entry of contact insecticides.” *Nature* 156: 112.

Qiu, Y., C. Tittiger, C. Wicker-Thomas, G. Le Goff, S. Young, E. Wajnberg, T. Fricaux, N. Taquet, G. J. Blomquist and R. Feyereisen (2012). “An insect-specific P450 oxidative

decarbonylase for cuticular hydrocarbon biosynthesis.” Proc Natl Acad Sci U S A 109(37): 14858-14863.

Ramsey (1935). “The evaporation of water from the cockroach.” Journal of Experimental biology 12: 373-383.

Rourke, B. C. and A. G. Gibbs (1999). “Effects of lipid phase transitions on cuticular permeability: model membrane and in situ studies.” J Exp Biol 202 Pt 22: 3255-3262.

Theisen, M. O., G. C. Miller, C. Cripps, M. Derenobales and G. J. Blomquist (1991). “Correlation of Carbaryl Uptake with Hydrocarbon Transport to the Cuticular Surface during Development in the Cabbage-Looper, *Trichoplusia-Ni*.” Pesticide Biochemistry and Physiology 40(2): 111-116.

Ugur, B., K. C. Chen and H. J. Bellen (2016). “*Drosophila* tools and assays for the study of human diseases.” Disease Models & Mechanisms 9(3): 235-244.

Wang, Y. W., T. C. da Cruz, A. Pulfemuller, S. Gregoire, J. F. Ferveur and B. Moussian (2016). “INHIBITION OF FATTY ACID DESATURASES IN *Drosophila melanogaster* LARVAE BLOCKS FEEDING AND DEVELOPMENTAL PROGRESSION.” Archives of Insect Biochemistry and Physiology 92(1): 6-23.

Wigglesworth (1945). “The effect of respiratory pattern on water loss in desiccation-resistant *Drosophila melanogaster*.” Journal of Experimental biology 21: 97-114.

Young, H. P., J. K. Larabee, A. G. Gibbs and C. Schal (2000). “Relationship between tissue-specific hydrocarbon profiles and lipid melting temperatures in the cockroach *Blattella germanica*.” Journal of Chemical Ecology 26(5): 1245-1263.

Yu, Z. T., Y. W. Wang, X. M. Zhao, X. J. Liu, E. B. Ma, B. Moussian and J. Z. Zhang (2017). “The ABC transporter ABCH-9C is needed for cuticle barrier construction in *Locusta migratoria*.” Insect Biochemistry and Molecular Biology 87: 90-99.

Appendix 1: Regionalization of surface lipids in insects

Wang, Yiwen; Yu, Zhitao; Zhang, Jianzhen; Moussian, Bernard (2016):

Regionalization of surface lipids in insects. In: *Proceedings. Biological sciences* 283 (1830). DOI: 10.1098/rspb.2015.2994.



Research

Cite this article: Wang Y, Yu Z, Zhang J, Moussian B. 2016 Regionalization of surface lipids in insects. *Proc. R. Soc. B* **283**: 20152994. <http://dx.doi.org/10.1098/rsob.2015.2994>

Received: 16 December 2015

Accepted: 12 April 2016

Subject Areas:

ecology, cellular biology

Keywords:

insect, cuticle, wetting, lipids, cuticular hydrocarbon

Author for correspondence:

Bernard Moussian

e-mail: bernard.moussian@unice.fr

[†]These authors contributed equally to this study.

Electronic supplementary material is available at <http://dx.doi.org/10.1098/rsob.2015.2994> or via <http://rsob.royalsocietypublishing.org>.

Regionalization of surface lipids in insects

Yiwen Wang^{1,2,†}, Zhitao Yu^{3,†}, Jianzhen Zhang³ and Bernard Moussian^{4,5}

¹Animal Genetics, Eberhard-Karls University of Tübingen, Auf der Morgenstelle 15, Tübingen 72076, Germany

²Robert-Bosch Krankenhaus, Institut für Klinische Pharmakologie, Auerbachstrasse 112, Stuttgart 70376, Germany

³Institute of Applied Biology, College of Life Science, Shanxi University, Taiyuan, Shanxi 030006, People's Republic of China

⁴Applied Zoology, Technical University Dresden, Zellescher Weg 20b, Dresden 01217, Germany

⁵IBV, Université Nice Sophia-Antipolis, Parc Valrose, Nice 06108, France

Cuticular hydrocarbons (CHCs) play a critical role in the establishment of the waterproof barrier that prevents dehydration and wetting in insects. While rich data are available on CHC composition in different species, we know little about their distribution and organization. Here, we report on our studies of the surface barrier of the fruit fly *Drosophila melanogaster* applying a newly developed Eosin Y staining method. The inert Eosin Y penetrates different regions of the adult body at distinct temperatures. By contrast, the larval body takes up the dye rather uniformly and gradually with increasing temperature. Cooling down specimens to 25°C after incubation at higher temperatures restores impermeability. Eosin Y penetration is also sensitive to lipid solvents such as chloroform indicating that permeability depends on CHCs. As in *D. melanogaster* adult flies, Eosin Y penetration is regionalized in *Tenebrio molitor* larvae, whereas it is not in *Locusta migratoria* nymphs. Regionalization of the fly surface implies tissue-specific variation of the genetic or biochemical programmes of CHC production and deposition. The Eosin Y-based map of CHC distribution may serve to identify the respective factors that are activated to accommodate ecological needs.

1. Introduction

An impermeable cuticle, which protects insects against dehydration and wetting, is probably one of the most important reasons for successful radiation of insects into almost every terrestrial niche. Free cuticular hydrocarbons (CHCs) covering the surface of the animal are believed to play a critical role in the establishment of this barrier [1]. An insect may harbour more than 100 different CHCs that are easily extracted with organic solvents like hexane or chloroform [2–4]. They range from simple *n*-alkanes to unsaturated and methyl-branched compounds [1,2,5]. The CHC composition, which is species-specific, is proposed to define the melting temperature (T_m) of the CHC layer that according to the lipid-melting model of Ramsey [6] correlates with the critical temperature (T_c) above which water is lost dramatically, leading to death [6–13]. Sudden increase in water loss above the T_c value is believed to rely on the conversion of CHCs from an impermeable solid state to a permeable fluid state [6,12,14,15]. Interestingly, CHC compositions are not uniform over the complete cuticle of an animal, the T_m can therefore differ from region to region [16].

Detailed analyses of whole body and body region T_c and T_m are particularly effective in large insects, such as locusts and cockroaches [8,16]. Fourier transform infrared (FTIR) spectrometers, for instance, allow studying lipid properties in cuticular lipids extracted from individuals or isolated organs in some insect species like *Tenebrio molitor* (mealworm), *Melanoplus sanguinipes* (grasshopper) and *Allonemobius fasciatus* (cricket) [12,16,17]. By contrast, the small body size of many insect species such as *Drosophila melanogaster* can hamper this type of work. Indeed, the available amount of CHCs from one individual small animal or parts of it may often be insufficient for analyses. Experiments using a mix of individuals cause loss of information on variations between individuals [12,18–20].

The ecological impact of CHCs has been well investigated in the *Drosophila* genus. A comparison between 18 different *Drosophila* species did not reveal any convincing correlation between CHC composition and temperature-dependent water loss [21]. Likewise, in the desert fruit fly *D. mojavensis*, changes in CHC amounts and composition in response to temperature increase did not improve desiccation resistance [22]. By contrast, desiccation-selected *D. melanogaster* had longer CHCs than control flies suggesting that higher T_m may contribute to reduced water loss [23]. Overall, however, at least in the genus *Drosophila*, the major adaptive mechanism to minimize water loss is to adjust gas exchange via the respiratory system [21]. Hence, besides their minor role in desiccation resistance, CHCs have other functions that are modulated during niche adaptation and evolution. One of these functions is their well-perceived influence on mating behaviour as sex pheromones [24].

Together with cuticle surface nano- and microstructures [25,26], the CHC surface layer is also involved in avoiding wetting, a serious hazard that may compromise respiration and locomotion [3]. This aspect is, despite its importance, marginally studied. In particular, the impact of temperature on cuticle wettability has not been addressed.

Here, we present a new *in situ* method designed to analyse the barrier function of the CHC layer in dependence of the temperature. Instead of assessing water loss at different temperatures, a common method in CHC research, by light microscopy, we study the ability of the animal to take up the inert dye Eosin Y reflecting cuticle barrier function at the tissue level. In the strict sense, of course, we cannot exclude that other cuticle components than CHC are responsible for the effects that we observed in this project. This method is applicable to the fruit fly *D. melanogaster*, to the locust *Locusta migratoria* and to the mealworm *T. molitor*, suggesting that it probably can be applied to all insects.

2. Material and methods

(a) Insects and Eosin Y staining

In principle, insects were initially stained at the rearing temperature (i.e. 25°C for *D. melanogaster* and *T. molitor*, and 30°C for *L. migratoria*). We next chose temperatures at and around the T_m or T_c values published: 30°C (T_m [21]) for *D. melanogaster* (T_c unknown), 50–60°C (T_c [8]) for *T. molitor* and 48°C (T_c [9]) for *L. migratoria*. Generally, negative staining results prompted us to increase the dye incubation temperature, which, on the contrary, was decreased after positive staining results.

To stain adult flies, 2–3-day-old w^{1118} flies were anaesthetized with CO₂ and transferred into a 2 ml microcentrifuge tube containing 1 ml dye solution (0.5% Eosin Y (W/V) and 0.1% Triton X-100) tempered at 4°, 18°, 25°, 30°, 37°, 40°, 45°, 50°, 55°, 58° or 60°C. After 20 min staining at the respective temperature, flies were washed three times with water (25°C) before microscopy. In the annealing experiment, flies were incubated for 20 min in water at 58°C. The whole tube was then cooled down on ice for 20 min. These flies were subsequently immersed in the dye solution at 25°C for 20 min. To remove surface lipids, 2 or 3 days old w^{1118} flies were anaesthetized with CO₂ and transferred into a 2 ml microcentrifuge tube containing 1 ml chloroform, hexane or heptane. After 2–3 min of incubation, flies were washed twice with water, and stained with Eosin Y solution at 25°C for 20 min. Thereupon, they were washed three times with water (25°C) and analysed immediately by microscopy. All incubation experiments were performed at least twice, each with 10 animals.

To obtain larvae for staining, *Oregon R* flies (WT) were kept at 25°C in egg laying cages on an apple juice agar plate garnished with a spot of fresh baker's yeast. Eggs were dechorionated in order to identify and collect late stage 17 embryos. These eggs were transferred to a new apple juice agar plate with yeast paste, and incubated at 18°C. Around twenty 24 h (L1) and 48 h (L2) old larvae were picked from the plate and transferred into 2 ml microcentrifuge tubes containing 200 µl water (25°C). One millilitre of 0.5% Eosin Y (W/V) preheated to 25°, 45°, 50° or 55°C was added to the tubes. Tubes were incubated at the indicated temperatures for further 30 min. Larvae were then washed three or four times with water (25°C) before microscopy. All incubation experiments were performed at least twice, each with more than 20 animals.

The mealworm larvae (Claus GmbH) with body lengths between 14 and 16 mm or pupae were transferred into a 2 ml microcentrifuge tube. One millilitre dye solution (0.5% Eosin Y (W/V) and 0.1% Triton X-100) preheated to 25°, 50°, 60°, 70°, 80° or 90°C was immediately added to the tubes. Tubes were incubated at the respective temperatures for 30 min. After incubation, the animals were washed three times with water (25°C). They were immediately analysed by microscopy. In total, five larvae or three pupae were tested at each temperature in two independent experiments.

To stain *L. migratoria* nymphs, eggs were incubated in a growth chamber (Yiheng, China) at 30°C under a relative humidity of 50%. First-instar nymphs without pigmentation were collected just after hatching. They were anaesthetized with CO₂ and transferred into a 2 ml microcentrifuge tube containing 1 ml dye solution (0.5% Eosin Y (W/V)) preheated to 30°, 45°, 48°, 50°, 53° or 55°C. Tubes were incubated at the respective temperature for further 30 min. Specimens were then washed three or four times with water (25°C) before microscopy. To remove surface lipids, we washed locusts with chloroform for 5 min. They were then incubated in Eosin Y solution for 10 min at room temperature (22°C). Before microscopy, animals were washed three or four times with water until the wash water was clear. All experiments were performed at least four times, each with two or three animals.

(b) Microscopy

A Leica MZ4 stereo-microscope with in-built camera was used for imaging large insects. Images were taken and details were observed using a Nikon AZ100 zoom microscope equipped with a Digital Sight DS-Fi1 camera. Images were formatted and prepared for publication with Adobe PHOTOSHOP and ILLUSTRATOR CS6 software.

3. Results

(a) Different parts of the fruit fly surface have different T_{pE} for Eosin Y

To illustrate cuticle impermeability, we first tested whether Eosin Y can penetrate the cuticle to stain the inside tissues of the animal at common temperatures of fruit fly breeding at 18°C and 25°C. At these two temperatures, most parts of the insects' surface were impermeable to Eosin Y (figure 1). Only two sensory organs on the head, the antennal and maxillary palps, were stained after 20 min immersion in the dye (figure 1; electronic supplementary material, figure S1). This shows that Eosin Y could penetrate the surface of these two organs. It is important to note that these results are generally independent from immersion time (data not show). Next, we stained animals at 4°C, and found that the antennal and maxillary palps did not stain. This result suggests that the permeability of the antennal and maxillary palps is temperature-dependent. Their critical temperature for Eosin Y penetration (T_{pE}) lies between 4°C and 18°C.

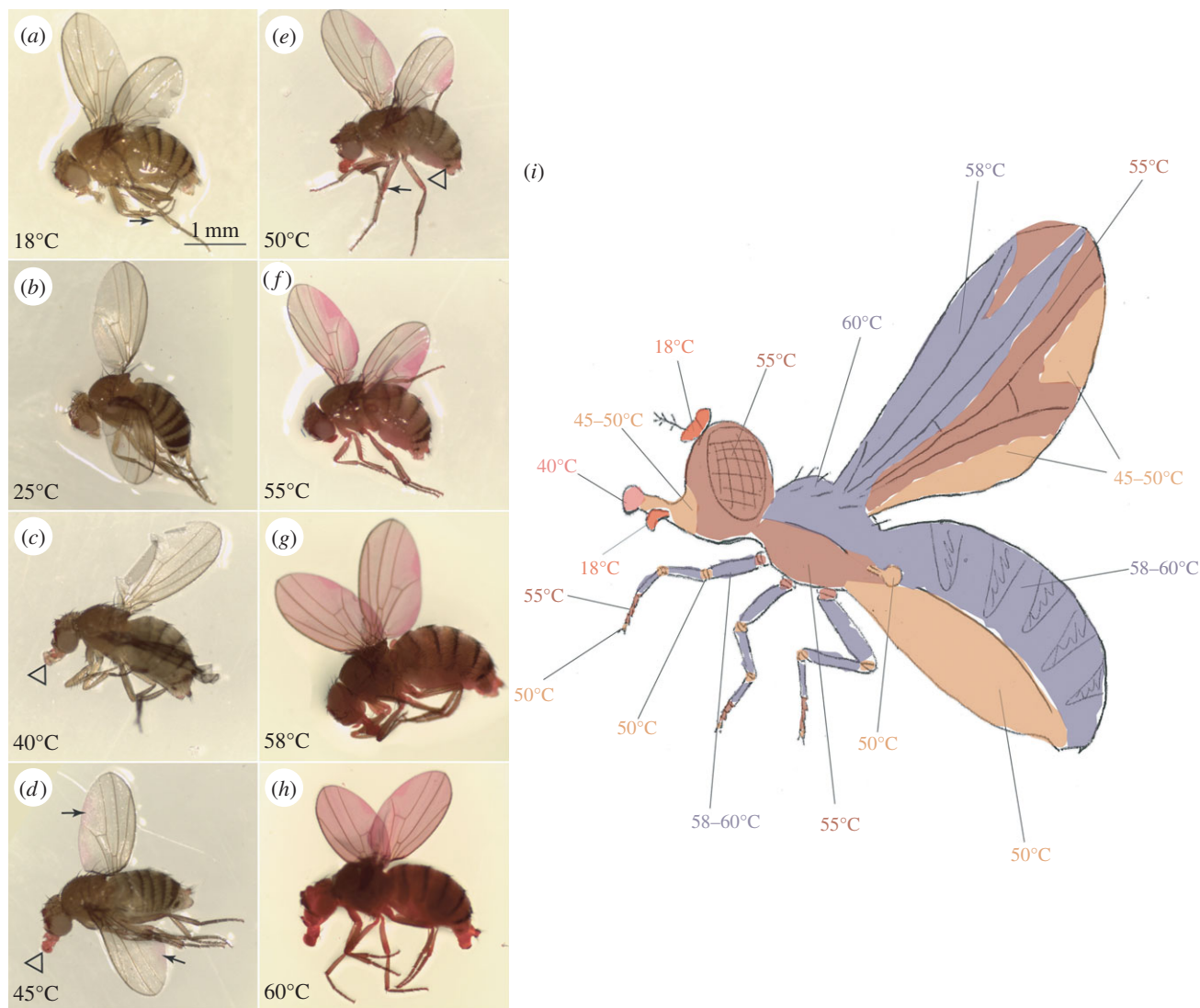


Figure 1. Eosin Y penetrates different parts of the fruit fly surface at different temperatures. Adult fruit flies were stained with Eosin Y at different temperatures. At low magnification, Eosin Y penetration is not visible at 18°C and 25°C (*a,b*). Dye penetration becomes first visible at 40°C in the proboscis (triangle, *c*). At 45°C, Eosin Y is taken up from the posterior edges of the wings (arrow, *d*). At 50°C, the Eosin Y signal intensifies and is also visible in the leg and (slightly) in the abdomen (arrow, *e*). At 55°C, the entire head and the wings are stained by Eosin Y (*f*). At 58°C, the whole body including the thorax is penetrated by Eosin Y (*g*). At 60°C, Eosin Y staining intensifies (*h*). These results are summarized in a cartoon (*i*).

We also studied the effects of temperatures higher than 25°C on cuticle permeability. Staining of the fly body with Eosin Y was unchanged at 30° (which corresponds roughly to the T_m value of 29°C [21]), 37° and 40°C (data not shown). In summary, as shown in figure 1 and electronic supplementary material figures S1 and S2, we found that different body regions became permeable to Eosin Y at distinct temperatures above 40°C. The dye started to penetrate the lower edge of the wing at 45°C, while it stained the wing's upper edge at 58°C (figure 1). Similarly, staining of the legs was non-uniform. The joints and the claws were first stained at 50°C (electronic supplementary material, figure S2), the tarsal segment at 55°C. Finally, the whole legs became red at 58°C (figure 1). By this method, some tissue-specific T_{PE} values could be determined exactly. For instance, the labellum remained impermeable until a temperature of 37°C, but became suddenly permeable to Eosin Y at 40°C.

To examine whether specimen treatment (particularly staining at higher temperatures) may injure the animals, thereby facilitating or enabling dye uptake, we cut wings or legs of wild-type flies before staining with Eosin Y (electronic

supplementary material, figure S3). Eosin Y was taken up locally at the wound site, but did not spread into the entire organ or body. Other possible entry sites for Eosin Y are the tracheal openings (spiracles). To answer the question whether these structures might be responsible for uncontrolled Eosin Y penetration, we microscopied the spiracles of the thorax and the abdomen after incubation in Eosin Y at 25° and 50°C (electronic supplementary material, figure S4). Eosin Y did not stain the spiracles at 25°C, but marked them at 50°C. The surrounding tissue, however, remained unstained. Thus, Eosin Y penetrates the fly body preferably through the cuticle.

In conclusion, Eosin Y incubation assays revealed a temperature-dependent regionalization of the fly surface for penetration of a hydrophilic molecule.

(b) Eosin Y penetration in the mealworm and locust cuticle is temperature-dependent

To evaluate the Eosin Y experiment with the fruit fly, we analysed Eosin Y penetration into the cuticle of *T. molitor* (mealworm) larvae and pupae, and freshly hatched

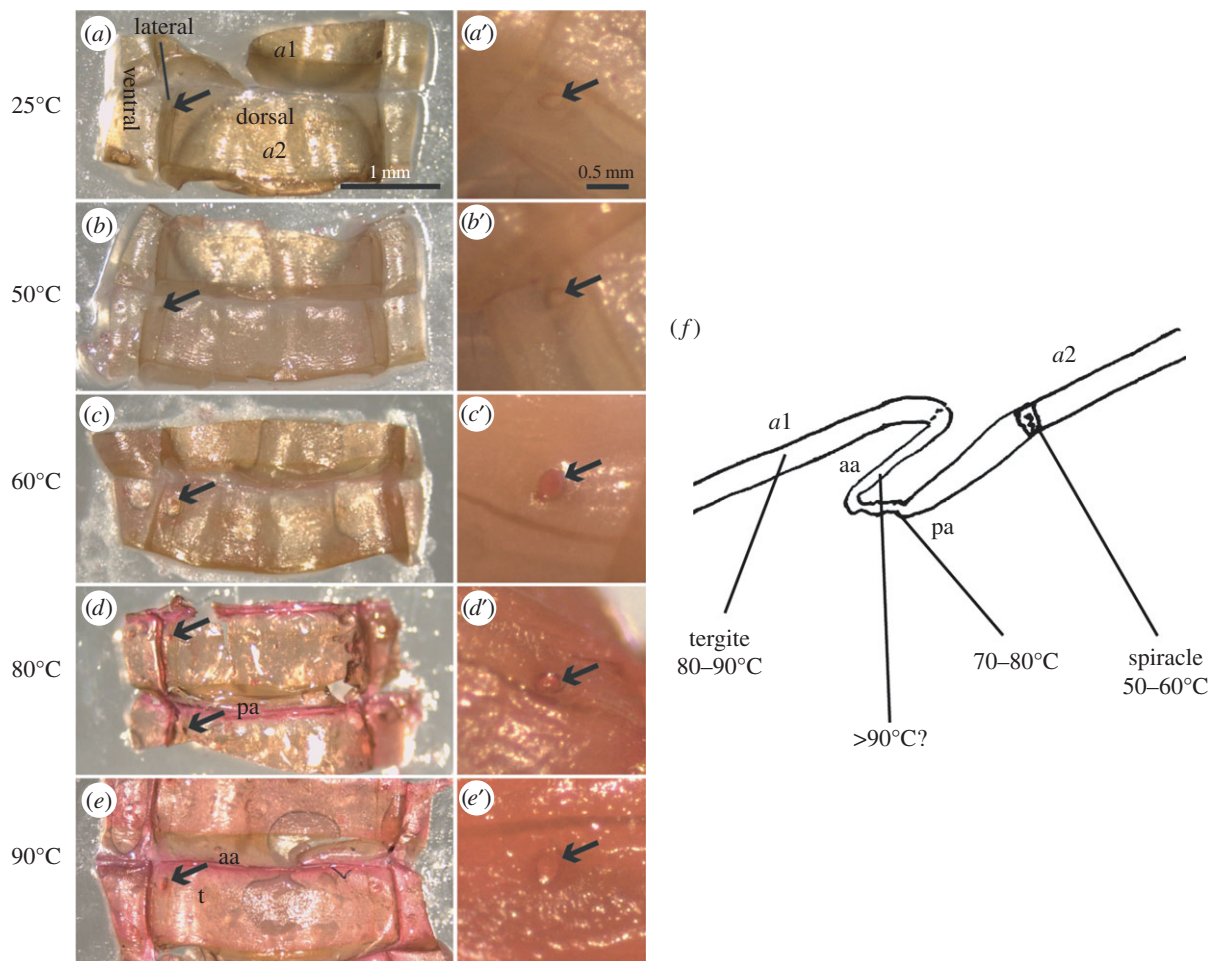


Figure 2. Eosin Y penetrates the cuticle of mealworm larva at high temperatures. At 25°C and 50°C, Eosin Y does not pass through the abdominal cuticle of mealworm larvae (*a–b'*). At 60°C, the spiracles (arrow) in the lateral cuticle of mealworm larvae take up Eosin Y, while other body parts remain unstained (*c, c'*). At 80°C, Eosin Y stains the posterior half of the arthroal membrane (*pa*) that connects the tergites (*d*). At 90°C, also the tergites (*t*) are stained by Eosin Y (*e*). Interestingly, the anterior half of the arthroal membrane (*aa*) remains unstained at this high temperature. These results are summarized in (*f*), showing a longitudinal section through the arthroal membrane (*aa* and *pa*) connecting abdominal segments 1 and 2. In (*a–e*), a dorsal view on two abdominal segments (1 and 2) is shown. The segments were unfolded after a cut at the ventral side.

first-instar nymphs of the locust *L. migratoria* at different temperatures (figures 2 and 3). Mealworm larvae have a high T_m value above 80°C [8,16]. Consistently, Eosin Y did not penetrate the cuticle of mealworm larvae at 25° and 50°C (figure 2). At 60°C, the spiracle became red, and the dye passed a bit into the body through the respiration system. This is comparable with the published T_c value of 50–60°C in larvae [8]. At 80°C, most soft parts of the cuticle became permeable to Eosin Y. At 90°C, Eosin Y stained also the sclerotized parts of the cuticle. Of note, the T_m value for *T. molitor* larval exuviae has been measured to be over 80°C [16]. Interestingly, the anterior part of the arthroal membrane was still impermeable at this high temperature. Pupae were completely impermeable to Eosin Y at 60°C. At 70°C, legs and the ventral side of the elytra and flight wings become red. Finally, at 80°C, the dye penetrated the whole pupa strongly (electronic supplementary material, figure S5). Hence, in *T. molitor* larvae and pupae the surface barrier against Eosin Y penetration is regionalized.

First-instar locust nymphs before pigmentation allowed easy scoring for staining with Eosin Y. Locusts were immersed in Eosin Y solution at 30°C, 45°C, 48°C, 50°C, 53°C or 55°C (figure 3). Eosin Y did not penetrate the cuticle at 30°C, which was the common temperature for locust husbandry. Likewise, at 45°C, most parts of the insects'

surface remained impermeable. By contrast, the insects' surface is slightly stained at 48°C. This is very close to the T_c value of 47°C determined for the adult locust [9]. Staining gradually intensified with an increase of the temperature to 55°C. Thus, together, in young locust nymphs surface seems not to be regionalized.

(c) The temperature-dependent permeability of fruit fly cuticle is reversible

To test whether the observed temperature-dependent permeability changes are reversible, we designed an annealing experiment. We heated the flies to 58°C for 20 min, cooled them slowly down on ice and immersed them for 20 min in Eosin Y at 25°C. These flies were not stained by Eosin Y, just like flies that were directly immersed in Eosin Y at 25°C without pre-heating (figure 4). This result indicates that temperature-dependent cuticle permeability is reversible.

We applied this method also to *D. melanogaster* L1 and L2 larvae. Both L1 and L2 larvae started to take up Eosin Y through their skin at 50°C (electronic supplementary material, figure S6). They were completely stained red at 55°C. In contrast to the situation in adult flies, cuticle impermeability of these larvae can only be partially restored.

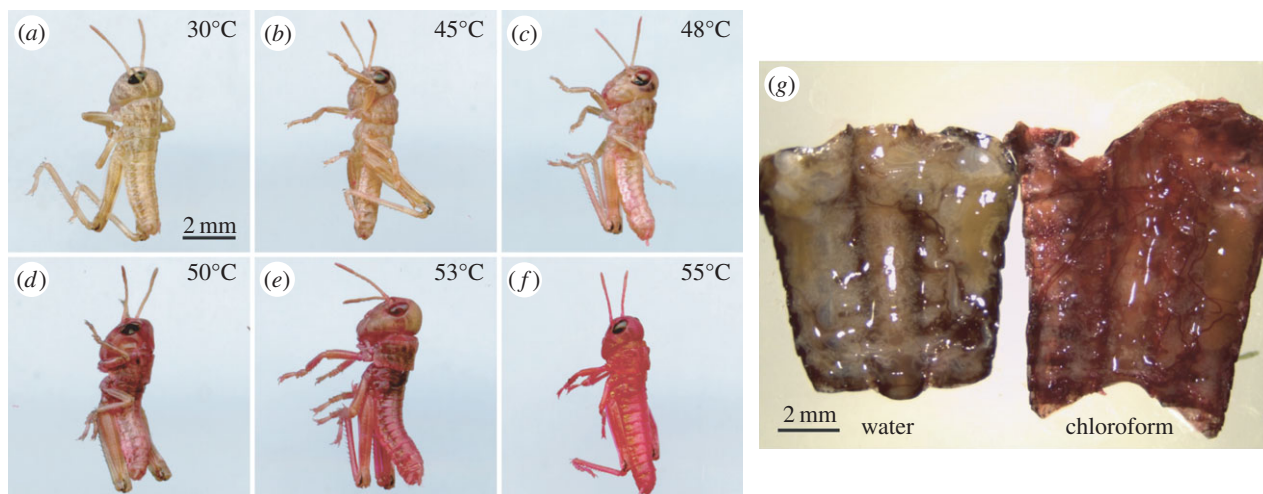


Figure 3. The surface of the locust nymph is not regionalized. At 30°C, Eosin Y does not penetrate the locust nymph cuticle (a). At 45°C, the body of the young nymph is slightly red after incubation in Eosin Y (b). Penetration of Eosin Y enhances gradually from 48°C (c), over 50°C (d) and 53°C (e) to 55°C (f). Chloroform wash at 25°C also enhances Eosin Y penetration into third instar nymphs (g).

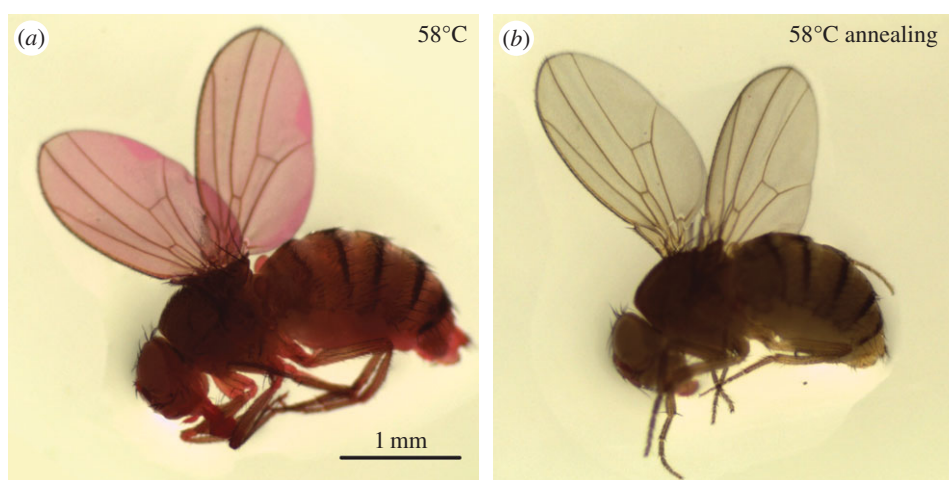


Figure 4. Heat-induced permeability to Eosin Y is reversible. Incubation with Eosin Y at 58°C (a). Flies that were heated up to 58°C and subsequently cooled down on ice (annealing) repel Eosin Y (b).

In summary, the *D. melanogaster* cuticle is a temperature-sensitive barrier for hydrophilic molecules that is better developed in adult flies than in larvae.

(d) Cuticle impermeability is overcome by washing with lipid solvents

We next investigated whether cuticle impermeability is due to the CHC layer at the surface of the animal. For this purpose, we stained flies with Eosin Y after washing them with chloroform, hexane and heptane, three lipid solvents that are traditionally used to extract insect surface lipids. We found that all solvents can systematically annihilate cuticle impermeability. Chloroform showed the strongest effect. Flies incubated with Eosin Y took in the dye acutely, becoming dark red, while hexane- or heptane-washed flies became light red. The difference was especially obvious in the wings, legs and halteres (figure 5). As in the fruit fly, chloroform application enabled Eosin Y penetration in locust nymphs. Thus, the surface barrier in locust nymphs seems to involve CHCs.

To independently test the role of CHCs in Eosin Y barrier formation, we stained fruit flies that were homozygous mutant for the *claret* (*ca*) gene coding for a regulator of lipid transport [27,28]. The entire wings of *ca* flies were red already at 55°C,

whereas only the posterior part of wild-type wings became red at this temperature (electronic supplementary material, figure S7). The premature uptake of Eosin Y was found in flies homozygous for either of two independent mutant alleles, *ca*¹ and *ca*^{msd}, supporting the conclusion that *ca* is needed for CHC deposition in the wing. These results also support the conclusion that the surface barrier is based on CHCs.

4. Discussion

The insect cuticle is a barrier against dehydration, at the same time preventing penetration of potentially harmful substances. Here, we report on the visualization of the temperature-dependent collapse of cuticle resistance to the inert dye Eosin Y in different insect species. Our work allows us to draw two conclusions and to formulate one hypothesis.

(a) First conclusion: Eosin Y penetration is blocked by cuticular hydrocarbons

At 58°C, Eosin Y, a red inert dye with molecular weight of 648 Da, penetrates the entire cuticle of the *D. melanogaster* imago. Comparable results were obtained with *L. migratoria*

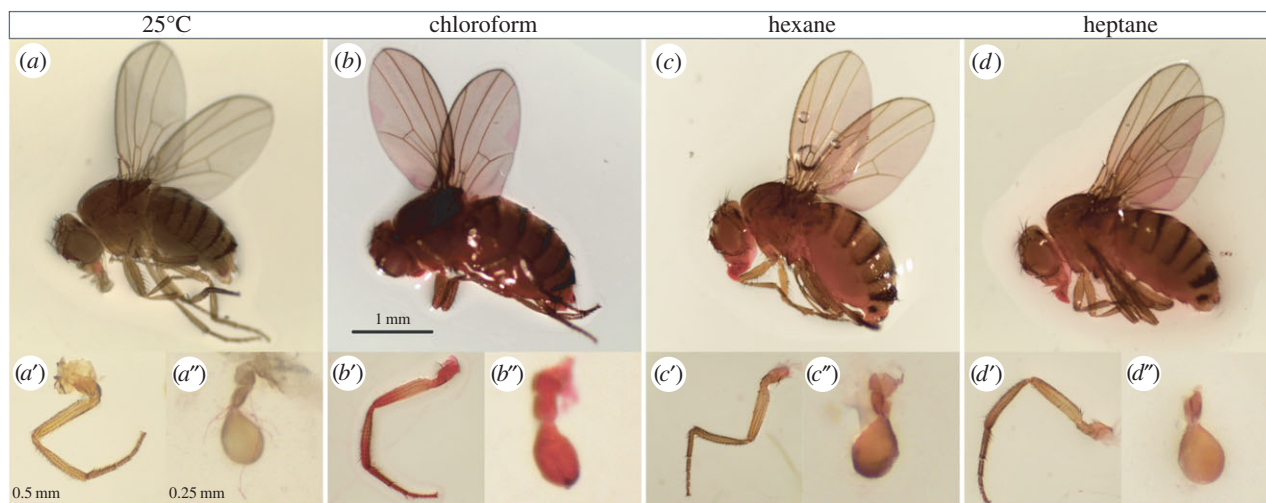


Figure 5. Lipid solvents enhance Eosin Y penetration into flies. At 25°C, at high magnification, Eosin Y barely penetrates the fly body (a). The fly becomes permeable after incubation of the fly in chloroform (b), hexane (c) and heptane (d). As exemplified for the legs (a', b', c', d') and the halteres (a'', b'', c'', d''), the effect is strongest after chloroform incubation.

and *T. molitor*. After incubation in chloroform, a solvent often used to extract surface lipids in insects, Eosin Y penetrates the entire adult cuticle of the adult fly and the locust nymph already at 25°C. Consistently, flies mutant for *ca* that codes for a GTPase required for lipid transport have a weaker barrier against Eosin Y penetration. The wings of these flies become red already at 55°C upon Eosin Y staining. These observations hint at a lipid-, possibly CHC-dependent mechanism of Eosin Y penetration protection, naturally, without excluding that other cuticle components (e.g. proteins might be involved). In the literature, there are only a few comprehensive reports on the function of CHCs in blocking penetration of hydrophilic substances into the arthropod cuticle [25,29]. Commonly, the surface nano- and micro-morphology of the cuticle is also considered as an important entity that prevents wetting [26,30–32]. In this work, we have not studied the effects of temperature and lipid solvents on the surface nanostructures of *D. melanogaster*, *L. migratoria* or *T. molitor* in Eosin Y staining experiments. However, we think that the restoration of cuticle impermeability in flies cooled down after heat treatment implies a simple, CHC-involving annealing mechanism rather than the reconstitution of a complex cuticular nanostructure. To corroborate this assumption, along with ultra-structural analyses of the insect surface, CHC composition and abundance before and after annealing have to be determined by gas chromatography and mass spectrometry. Together, our data nevertheless suggest that Eosin Y penetration depends on surface lipids (i.e. CHCs that change their aggregate state at the utmost at 58°C in *D. melanogaster*).

(b) Second conclusion: Eosin Y application reveals body surface regionalization in *Drosophila melanogaster* and *Tenebrio molitor*

Different regions of the *D. melanogaster* adult fly surface become permeable to Eosin Y at different temperatures. Likewise, Eosin Y penetrates different parts of the cuticle of mealworm larvae at distinct temperatures. These findings indicate that different regions of the insect surface are composed of specific structural and chemical factors including

CHCs. This conclusion is in agreement with recent mass spectrometric data on the distribution of neutral lipids on the surface of *D. melanogaster* [33]. Combining mass spectrometry with laser-assisted ionization imaging, among others, it was shown that different lipids cover the anterior and posterior halves of the wing. This mirrors our finding that the Eosin Y is soaked in by the anterior half of the wing at a higher temperature than by its posterior half. Moreover, the melting temperatures of CHCs of different body parts of the grasshopper *Melanoplus sanguinipes*, a large insect, have been demonstrated by FTIR spectroscopy to vary [16]. Conceivably, regionalization of the insect surface suggests region-specific genetic programmes deployed during cuticle development or reparation. In principle, the notion of surface regionalization is in line with the hypothesis of spatial separation of lipid phases on the cuticle formulated by Allen Gibbs in 2002 [13]. He postulated spatially different distribution of surface lipids (especially of high-melting alkanes) in order to explain why water loss rates do not correlate perfectly with the measured 'bulk' lipid-melting point. Thanks to the arsenal of molecular and genetic tools available, including tissue-specific gene silencing methods [34], *D. melanogaster* is the perfect model insect to uncover the respective underlying genetic and molecular factors.

In contrast to the situation in *D. melanogaster* adults and *T. molitor* larvae, the surface of locust first-instar nymphs and *D. melanogaster* larvae is not regionalized. How can these cases be explained in the light of the data discussed above? In the case of *D. melanogaster*, it may be that larvae as relatively simple life forms with limited behavioural repertoire and a uniform soft cuticle (note that the hard head skeleton is inverted) do not require differential CHC distribution for communication with the environment or survival. Comparably, body organization in alternating soft and hard cuticle types in *T. molitor* larvae is mirrored by differential distribution of CHCs. In the case of locust nymphs, it may simply be that freshly hatched and unpigmented nymphs have not yet developed an elaborate CHC coat. Although highly speculative at the moment, it may also be that a differential CHC distribution has not evolved in the more ancestral hemimetabolous insect species such as *L. migratoria*, but has in holometabolous

insects (*T. molitor*, *D. melanogaster*) [35,36]. Of course, it is equally possible that simplification of CHC distribution in locusts is a derived trait. These possibilities shall be tested in appropriate staining experiments using older animals and additional species representing different taxa and modes of life.

In any case, the Eosin Y penetration method established for *D. melanogaster*, *T. molitor* larvae and *L. migratoria* nymphs may potentially be used to plot maps of the surface of any insect of interest. These maps, in turn, may serve to study the mode of action of contact insecticides or any other lipophilic substance that interact with cuticular lipids in pest insects. Contact insecticides such as cypermethrin, sumithion, dieldrin and carbaryl [37–40] may associate with a preferred region-specific composition of CHCs. Indeed, in the case of dieldrin, distribution of the insecticide within the body of cockroaches (*Periplaneta americana*) was more effective after application on the pronotum than on the wing [37]. The pulvilli of tsetse flies (*Glossina spp.*) have been found to be very effective in DTT and glyrethrum uptake [41]. Beyond that, diflubenzuron and flufenoxuron, two derivatives of the lipophilic benzoylurea-based chitin synthesis inhibitors, pass through the bumblebee (*Bombus terrestris*) cuticle with different efficiencies [42]. Taking these arguments together, knowledge about the preferred region of cuticle penetration and identification of the respective CHCs may help to optimize the impact of an insecticide by chemical modifications. Ultimately, uptake optimization might result in the development of species-specific insecticides.

(c) Hypothesis: Eosin Y penetration mirrors anti-wetting barrier constitution

Eosin Y penetrates the surface of different body regions at respective temperatures ranging from 18°C to 58°C. Except for the T_{PE} measured for parts of the head, the T_{PE} values of the other body parts are higher than the lipid-melting temperature T_m of around 29°C determined for *D. melanogaster* [21]. To what extent is it reasonable to compare T_{PE} with T_m ? Or would we compare apples and oranges? Indeed, T_{PE} characterizes the outside-in (penetration) barrier, whereas T_m describes a property of the inside-out (transpiration) barrier that relies largely on CHCs. As reckoned in our first conclusion (see above), our results collectively suggest that CHCs may also be responsible for the penetration barrier. Considering hence CHCs as the central element of both types of barrier, we conjecture two alternative explanations for the discrepancy between T_m and most T_{PE} values in *D. melanogaster*. First, in a simple scenario, the size of the molecule that is able to pass through the CHC layer is directly proportional to the temperature that influences the physical properties of the barrier. Water, a small molecule, diffuses through the CHC barrier at moderate, physiological temperatures around the melting

and critical temperatures [13,21]. Bigger molecules (Eosin Y, 648 Da) are retained at these temperatures, but pass through the CHC layer at higher temperatures. Application of other dyes with different sizes in similar experiments described here should serve to challenge this possibility.

Second, admittedly a less probable scenario, transpiration (water) and penetration (Eosin Y) may rely on distinct properties of the CHC layer. In other words, T_m and T_{PE} reflect distinct characteristics of the CHC layer. Wetting, a prerequisite for penetration, occurs at higher temperatures than transpiration and is independent of CHC melting in this scenario. Interestingly, T_{PE} values in some parts of the head, where many sensory organs are placed, are low, enabling communication with the environment. By contrast, they are not physiological in the other body regions suggesting that CHCs seal these regions perfectly against penetration at physiological conditions beyond necessity.

Previously, it was shown that T_m values of CHCs in species of the *Drosophila* genus living in mesic or xeric habitats are around 30°C irrespective of the habitat. This suggests a similar CHC composition in these species. Our aim is to scrutinize whether the T_{PE} values of these species are also similar.

(d) Concluding remarks

Regionalization of the insect penetration barrier is probably reflected by the differential distribution of CHCs. In order to identify the region-specific CHC species, we propose to combine our Eosin Y staining method with the method of solid-phase micro-extraction (SPME) prior to gas chromatography and mass spectrometry (GC-MS). Indeed, SPME-GC-MS has been applied successfully for the identification of CHCs on single insects [43–45].

Finally, we should consider that surface regionalization described and discussed here may be specific to Eosin Y. Using our approach, the behaviour of other inert dyes like bromophenol blue should be tested for a generalized statement.

Ethics. All experiments described here were performed according to local guidelines. Appropriate ethical approval and licences were obtained.

Data accessibility. All data from this work will be publicly available in the Dryad Digital Repository <http://dx.doi.org/10.5061/dryad.kk52g>.

Authors' contributions. B.M. and Y.W. conceived and designed the experiments. Y.W. and Z.Y. performed the experiments. All authors analysed and discussed the data and wrote the manuscript and approved the final version.

Competing interests. All authors declare that they have no competing interests.

Funding. This work was supported by the DFG (grant MO1714/6) and the ICEPHA graduate programme (<http://www.icepha.de/icepha-graduate-program/projects.html>).

References

- Blomquist GJ, Bagnères A-G. 2010 *Insect hydrocarbons: biology biochemistry and chemical ecology*. Cambridge, UK: Cambridge University Press.
- Blomquist GJ, Nelson DR, Derenobales M. 1987 Chemistry, biochemistry, and physiology of insect cuticular lipids. *Arch. Insect Biochem.* **6**, 227–265. (doi:10.1002/arch.940060404)
- Lockey KH. 1988 Lipids of the insect cuticle—origin, composition and function. *Comp. Biochem. Phys. B* **89**, 595–645. (doi:10.1016/0300-9629(88)90839-0)
- Gibbs AG. 1998 Water-proofing properties of cuticular lipids. *Am. Zool.* **38**, 471–482. (doi:10.1093/icb/38.3.471)
- Patel S, Nelson DR, Gibbs AG. 2001 Chemical and physical analyses of wax ester properties. *J. Insect Sci.* **1**, 4. (doi:10.1673/031.001.0401)
- Ramsey JA. 1935 The evaporation of water from the cockroach. *J. Exp. Biol.* **12**, 373–383.
- Beament JWL. 1945 The cuticular lipoids of insects. *J. Exp. Biol.* **21**, 115–131.

8. Wigglesworth VB. 1945 Transpiration through the cuticle of insects. *J. Exp. Biol.* **21**, 97–114.
9. Loweridge JP. 1968 Control of water loss in *Locusta migratoria migratorioides* R + F. I. Cuticular water loss. *J. Exp. Biol.* **49**, 1–13.
10. Loweridge JP. 1968 Control of water loss in *Locusta migratoria migratorioides* R and F O.2. Water loss through spiracles. *J. Exp. Biol.* **49**, 15–29.
11. Davis MT. 1974 Critical temperature and changes in cuticular lipids in the rabbit tick, *Haemaphysalis leporispalustris*. *J. Insect Physiol.* **20**, 1087–1100. (doi:10.1016/0022-1910(74)90150-4)
12. Rourke BC, Gibbs AG. 1999 Effects of lipid phase transitions on cuticular permeability: model membrane and in situ studies. *J. Exp. Biol.* **202**, 3255–3262.
13. Gibbs AG. 2002 Lipid melting and cuticular permeability: new insights into an old problem. *J. Insect Physiol.* **48**, 391–400. (doi:10.1016/S0022-1910(02)00059-8)
14. Yoder JA, Benoit JB, Rellinger EJ, Ark JT. 2005 Critical transition temperature and activation energy with implications for arthropod cuticular permeability. *J. Insect Physiol.* **51**, 1063–1065. (doi:10.1016/j.jinsphys.2005.06.002)
15. Gibbs AG. 2011 Thermodynamics of cuticular transpiration. *J. Insect Physiol.* **57**, 1066–1069. (doi:10.1016/j.jinsphys.2011.05.003)
16. Gibbs A, Crowe JH. 1991 Intraindividual variation in cuticular lipids studied using Fourier-transform infrared-spectroscopy. *J. Insect Physiol.* **37**, 743–748. (doi:10.1016/0022-1910(91)90108-C)
17. Young HP, Larabee JK, Gibbs AG, Schal C. 2000 Relationship between tissue-specific hydrocarbon profiles and lipid melting temperatures in the cockroach *Blattella germanica*. *J. Chem. Ecol.* **26**, 1245–1263. (doi:10.1023/A:1005440212538)
18. Gibbs A, Mousseau TA, Crowe JH. 1991 Genetic and acclimatory variation in biophysical properties of insect cuticle lipids. *Proc. Natl Acad. Sci. USA* **88**, 7257–7260. (doi:10.1073/pnas.88.16.7257)
19. Gibbs A, Mousseau TA. 1994 Thermal-acclimation and genetic-variation in cuticular lipids of the lesser migratory grasshopper (*Melanoplus sanguinipes*)—effects of lipid-composition on biophysical properties. *Physiol. Zool.* **67**, 1523–1543. (doi:10.1086/physzool.67.6.30163910)
20. Rourke BC. 2000 Geographic and altitudinal variation in water balance and metabolic rate in a California grasshopper, *Melanoplus sanguinipes*. *J. Exp. Biol.* **203**, 2699–2712.
21. Gibbs AG, Fukuzato F, Matzkin LM. 2003 Evolution of water conservation mechanisms in *Drosophila*. *J. Exp. Biol.* **206**, 1183–1192. (doi:10.1242/jeb.00233)
22. Gibbs AG, Louie AK, Ayala JA. 1998 Effects of temperature on cuticular lipids and water balance in a desert *Drosophila*: is thermal acclimation beneficial? *J. Exp. Biol.* **201**, 71–80.
23. Gibbs AG, Chippindale AK, Rose MR. 1997 Physiological mechanisms of evolved desiccation resistance in *Drosophila melanogaster*. *J. Exp. Biol.* **200**, 1821–1832.
24. Bontonou G, Wicker-Thomas C. 2014 Sexual Communication in the *Drosophila* genus. *Insects* **5**, 439–458. (doi:10.3390/insects5020439)
25. Holdgate MW. 1955 The wetting of insect cuticles by water. *J. Exp. Biol.* **32**, 591–617.
26. Darmanin T, Guittard F. 2015 Superhydrophobic and superoleophobic properties in nature. *Mater. Today* **18**, 273–285. (doi:10.1016/j.mattod.2015.01.001)
27. Ma J, Plesken H, Treisman JE, Edelman-Novemsky I, Ren M. 2004 Lightoid and Claret: a rab GTPase and its putative guanine nucleotide exchange factor in biogenesis of *Drosophila* eye pigment granules. *Proc. Natl Acad. Sci. USA* **101**, 11 652–11 657. (doi:10.1073/pnas.0401926101)
28. Wang C, Liu Z, Huang X. 2012 Rab32 is important for autophagy and lipid storage in *Drosophila*. *PLoS One* **7**, e32086. (doi:10.1371/journal.pone.0032086)
29. Ghiradel H, Radigan W. 1974 Collembolan cuticle—wax layer and anti-wetting properties. *J. Insect Physiol.* **20**, 301–306. (doi:10.1016/0022-1910(74)90062-6)
30. Sun M, Watson GS, Zheng Y, Watson JA, Liang A. 2009 Wetting properties on nanostructured surfaces of cicada wings. *J. Exp. Biol.* **212**, 3148–3155. (doi:10.1242/jeb.033373)
31. Sun M, Liang A, Watson GS, Watson JA, Zheng Y, Ju J, Jiang L. 2012 Influence of cuticle nanostructuring on the wetting behaviour/states on cicada wings. *PLoS ONE* **7**, e35056. (doi:10.1371/journal.pone.0035056)
32. Gundersen H, Leinaas HP, Thaulow C. 2014 Surface structure and wetting characteristics of *Collembola* cuticles. *PLoS ONE* **9**, e86783. (doi:10.1371/journal.pone.0086783)
33. Kaftan F, Vrkoslav V, Kynast P, Kulkarni P, Bocker S, Cvacka J, Knaden M, Svatos A. 2014 Mass spectrometry imaging of surface lipids on intact *Drosophila melanogaster* flies. *J. Mass Spectrom.* **49**, 223–232. (doi:10.1002/jms.3331)
34. Mohr SE. 2014 RNAi screening in *Drosophila* cells and in vivo. *Methods* **68**, 82–88. (doi:10.1016/j.ymeth.2014.02.018)
35. Misof B *et al.* 2014 Phylogenomics resolves the timing and pattern of insect evolution. *Science* **346**, 763–767. (doi:10.1126/science.1257570)
36. Cheong SP, Huang J, Bendena WG, Tobe SS, Hui JH. 2015 Evolution of ecdysis and metamorphosis in arthropods: the rise of regulation of juvenile hormone. *Integr. Comp. Biol.* **55**, 878–890. (doi:10.1093/icb/icv066)
37. Moriarty F, French MC. 1971 The uptake of dieldrin from cuticular surface of *Periplaneta americana* L. *Pest Biochem Physiol* **1**, 286–292. (doi:10.1016/0048-3575(71)90160-X)
38. Theisen MO, Miller GC, Cripps C, Derenobales M, Blomquist GJ. 1991 Correlation of carbaryl uptake with hydrocarbon transport to the cuticular surface during development in the cabbage-looper, *Trichoplusia-Ni*. *Pestic Biochem. Phys.* **40**, 111–116. (doi:10.1016/0048-3575(91)90105-U)
39. Juarez P. 1994 Inhibition of cuticular lipid-synthesis and its effect on insect survival. *Arch. Insect Biochem.* **25**, 177–191. (doi:10.1002/arch.940250302)
40. Lin YY, Jin T, Zeng L, Lu YY. 2012 Cuticular penetration of beta-cypermethrin in insecticide-susceptible and resistant strains of *Bactrocera dorsalis*. *Pestic Biochem. Phys.* **103**, 189–193. (doi:10.1016/j.pestbp.2012.05.002)
41. Potts WH, Vanderplank FL. 1945 Mode of entry of contact insecticides. *Nature* **156**, 112. (doi:10.1038/156112a0)
42. Mommaerts V, Sterk G, Smagge G. 2006 Hazards and uptake of chitin synthesis inhibitors in bumblebees *Bombus terrestris*. *Pest Manag. Sci.* **62**, 752–758. (doi:10.1002/ps.1238)
43. Tentschert J, Kolmer K, Holldobler B, Bestmann HJ, Delabie JH, Heinze J. 2001 Chemical profiles, division of labor and social status in *Pachycondyla* queens (Hymenoptera: formicidae). *Naturwissenschaften* **88**, 175–178. (doi:10.1007/s001140100218)
44. Golebiowski M, Bogus MI, Paszkiewicz M, Stepnowski P. 2011 Cuticular lipids of insects as potential biofungicides: methods of lipid composition analysis. *Anal. Bioanal. Chem.* **399**, 3177–3191. (doi:10.1007/s00216-010-4439-4)
45. Cerkowniak M, Puckowski A, Stepnowski P, Golebiowski M. 2013 The use of chromatographic techniques for the separation and the identification of insect lipids. *J. Chromatogr. B Analyt Technol. Biomed. Life Sci.* **937**, 67–78. (doi:10.1016/j.jchromb.2013.08.023)

Appendix 2: Double cuticle barrier in two global pests, the whitefly *Trialeurodes vaporariorum* and the bedbug *Cimex lectularius*.

Wang, Yiwen; Carballo, Rocio Gallego; Moussian, Bernard (2017): **Double cuticle barrier in two global pests, the whitefly *Trialeurodes vaporariorum* and the bedbug *Cimex lectularius***. In: *The Journal of experimental biology* 220 (Pt 8), S. 1396–1399. DOI: 10.1242/jeb.156679.

SHORT COMMUNICATION

Double cuticle barrier in two global pests, the whitefly *Trialeurodes vaporariorum* and the bedbug *Cimex lectularius*

Yiwen Wang¹, Rocío Gallego Carballo¹ and Bernard Moussian^{2,3,*}**ABSTRACT**

The integument protects the organism against penetration of xenobiotics and water that would potentially interfere with homeostasis. In insects that play key roles in a variety of agricultural and ecological habitats, this inward barrier has barely been investigated. In order to advance knowledge in this field, we studied integumental barrier (cuticle) permeability in the two global pests *Trialeurodes vaporariorum* (greenhouse whitefly) and *Cimex lectularius* (bedbug), applying a simple dye-penetration assay. In agreement with our recent findings in *Drosophila melanogaster*, we show that the surface of these insects is regionalised. We also show that, in contrast to the single barrier in *D. melanogaster*, two barriers with distinct temperature-sensitive and lipid-based physico-chemical material properties act in parallel to protect these insects against penetration of hydrophilic molecules. These findings imply the existence of unexplored mechanisms by which the cuticle acts as a protective coat against the penetration of water and xenobiotics, including pollutants and insecticides.

KEY WORDS: Cuticular hydrocarbon (CHC), Water, Xenobiotics**INTRODUCTION**

Generally, in most habitats, insects are in close contact with their wet or solid environment, running the risk of undesired uptake of water, solutes and toxic molecules. They erect a composite barrier – the cuticle – at the apical side of their epidermis that protects them against these hazards. The first, physical barrier in penetration protection is constituted by cuticle nanostructures and macrostructures protruding at their surface (Watson et al., 2010; Sun et al., 2012; Gundersen et al., 2014; Darmanin and Guittard, 2015). The material properties of the second inward barrier are to a large extent defined by lipophilic compounds including waxes and free cuticular hydrocarbons (CHCs) at the cuticle surface (Ramsay, 1935; Noble-Nesbitt, 1970; Gibbs, 1998; Rourke and Gibbs, 1999; Gibbs, 2002; Moussian, 2010; Gibbs, 2011). According to the lipid-melting model of Ramsay (1935), water flow across the cuticle depends on the temperature at which cuticular waxes and CHCs exhibit a phase transition from solid to fluid, termed the critical temperature (T_c). The T_c values vary between species (Gibbs, 2002). These compounds are transported to the surface via a cuticular canal system comprising pore and wax canals that are continuous with the apical plasma membrane of epidermal cells (Wigglesworth, 1975).

These canals are potential routes of uncontrolled penetration of water and solutes (Locke, 1965; Wigglesworth, 1986, 1990).

While cuticular microstructures and nanostructures are being analysed extensively (Darmanin and Guittard, 2015), the wax/CHC-based inward barrier of insects has not been studied in detail. A central problem in this field is to visualise penetration. Recently, we showed that the easily visualised harmless and water-soluble dye Eosin Y penetrates into the cuticle of several insect species dependent on lipid solvent-soluble CHCs and temperature (Wang et al., 2016). Interestingly, Eosin Y did not penetrate the surface uniformly, but at regionally different rates. We hypothesised that CHC composition is regionalised reflecting body region-specific physiological, and by consequence genetic, programmes. We reason that these differences may have an impact on the activity and efficiency of contact insecticides that are taken up by the cuticle. To study inward permeability patterns in the cuticle of insects with applied relevance, we used the Eosin Y penetration assay on various insect species. Here, we report on our analyses of the permeability barrier in two global human pests: the whitefly *Trialeurodes vaporariorum* Westwood 1856, a widespread greenhouse pest, and the human parasite bedbug *Cimex lectularius* Linnaeus 1758. Our data demonstrate that, as in *Drosophila melanogaster*, temperature-dependent permeability to Eosin Y is regionalised in these two species. In contrast to the situation in *D. melanogaster*, however, permeability in *T. vaporariorum* and *C. lectularius* is also regionalised after removal of surface lipids with chloroform. Similar results were obtained in penetration assays using other, chemically different dyes such as Bromophenol Blue and Methylene Blue. We infer that in contrast to *D. melanogaster*, two distinct barriers are present in the whitefly and bedbug cuticle.

MATERIALS AND METHODS**Animal husbandry and dye incubation**

Whitefly (*T. vaporariorum*) adults were obtained from Nuetzlinge.de (Ammerbuch, Germany) and Katz Biotech AG (Baruth/Mark, Germany). We focused on their wings, which are rather robust in handling compared to the rest of the whitefly body. Bedbugs (*C. lectularius*) that were reared at 22°C in plastic vials furnished with a filter paper were obtained from the Reinhardt laboratory at the TU Dresden (Reinhardt et al., 2003). Eosin Y staining followed the recently described procedure (Wang et al., 2016). In brief, animals were incubated in plastic vials at different temperatures in 1 ml 0.5% (w/v) Eosin Y and 0.1% Triton X-100 (both Sigma Aldrich) using standard thermo-shakers. Bromophenol Blue (Sigma, 0.5% w/v, 0.1% Triton X-100) and Methylene Blue (Sigma, 0.1% w/v, 0.1% Triton X-100) were applied following the same protocol. All three dyes are generally used in histology as unspecific detectors of a variety of molecules (Selman, 1960; Marconi and Quintana, 1998; Fischer et al., 2008). For chloroform washes, insects were incubated in the solvent for 2 min in glass vials prior to staining with dyes at respective temperatures.

¹Genetik der Tiere, Universität Tübingen, Auf der Morgenstelle 15, 72076 Tübingen, Germany. ²Angewandte Zoologie, TU Dresden, Zellescher Weg 20b, 01069 Dresden, Germany. ³IBV, Université Nice, Parc Valrose, Nice 06000, France.

*Author for correspondence (bernard.moussian@uni-tuebingen.de)

 B.M., 0000-0002-2854-9500

Microscopy and imaging

A Leica MZ4 stereo-microscope with in-built camera was used for imaging whole insects. Images were taken and details were observed using a Nikon AZ100 zoom microscope equipped with a Digital Sight DS-Fi1 camera. Images were formatted and prepared for publication with Adobe Photoshop and Illustrator CS6 software without manipulation of the initial settings of the microscopes.

RESULTS AND DISCUSSION

Eosin Y penetration in whiteflies depends on temperature and chloroform-soluble components

Eosin Y was excluded from the *T. vaporariorum* wing cuticle at 25 and 60°C (Fig. 1). Penetration of the dye started at 70°C. A broad area at the basis, the margin and the single wing vein was stained at 70°C, and the entire wing surface was stained at 80°C. Prolonged incubation of whiteflies in Eosin Y at 60 or 70°C did not alter the dye penetration pattern (Fig. S1) suggesting that lateral diffusion does not play a role in this process. Cooling down whiteflies from 80°C to 0°C prior to staining at 25°C prevented Eosin Y uptake. This result underlines that our staining method does not inflict wounds that would entail uncontrolled dye penetration. Together, these findings indicate that permeability of the wing cuticle to Eosin Y is temperature dependent and restorable. Barrier restoration, i.e. reversibility of high-temperature permeabilisation, allows us to exclude the involvement of surface microstructures and

nanostructures in Eosin Y repellence, assuming that cuticular structures are not temperature sensitive. Moreover, similar to the situation in the fruit fly *D. melanogaster* (Wang et al., 2016), whitefly wings are regionalised with respect to permeability to Eosin Y.

Next, we investigated the permeability properties of the wing cuticle surface with respect to Eosin Y penetration after incubation in chloroform, a widely used lipid solvent (Fig. 1). Eosin Y penetrated the wing margin and the wing vein after chloroform incubation, while the wing blade remained unstained. This finding suggests that permeability to Eosin Y is partially and regionally lipid dependent.

To further scrutinise the properties of the barrier against penetration in *T. vaporariorum*, we combined the effects of temperature with those of chloroform on permeability to Eosin Y (Fig. 1). After incubation in chloroform, Eosin Y stained the wing blade in addition to the wing margin at temperatures of 60°C and above. This observation indicates that the effects of temperature and chloroform on the penetration barrier are additive. In turn, this suggests that the penetration barrier consists of at least two different components, one of which is only sensitive to temperature, while the other is damageable by lipid solvents. The situation is even more complex, as staining of Eosin Y was uniform and did not intensify at 80°C regardless of chloroform treatment. Thus, the putative solvent-soluble component is also temperature sensitive but loses its barrier properties only at very

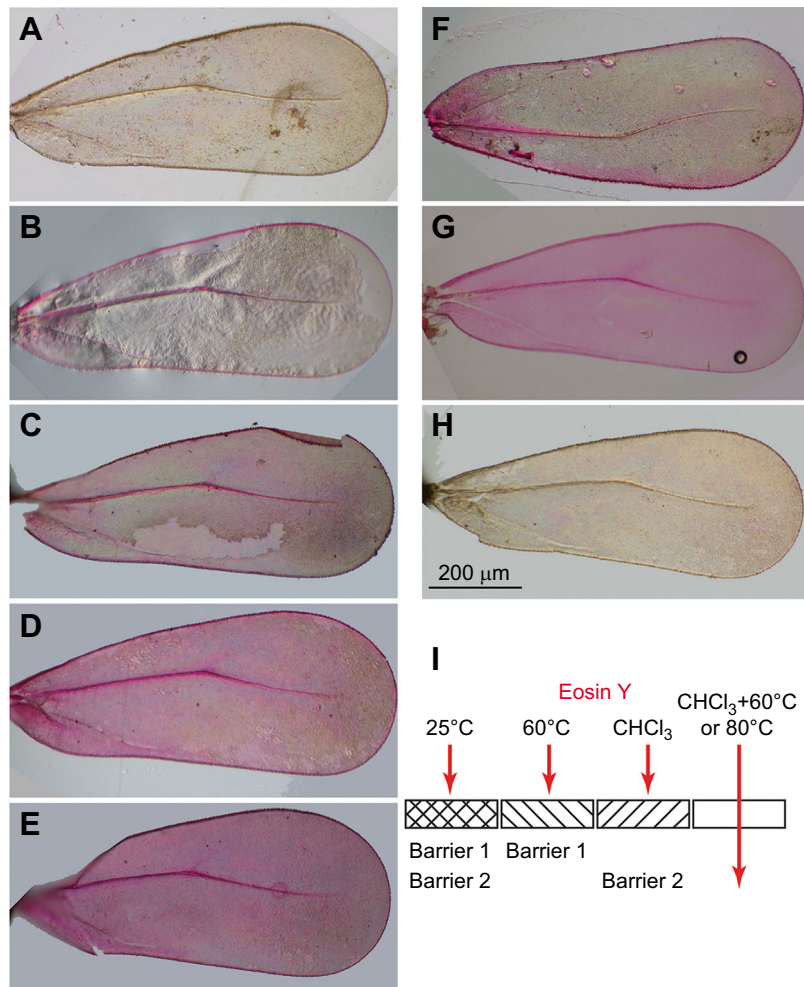


Fig. 1. Two cuticular barriers in *Trialeurodes*

vaporariorum. (A) Wings do not take up Eosin Y at 60°C. (B) Eosin Y penetrates the wing margin and vein after chloroform wash. (C) The entire wing is stained by Eosin Y when incubated at 60°C after chloroform wash. (D) The entire wing is red when stained at 80°C. (E) Staining at 80°C is not enhanced after chloroform wash. (F) At 70°C, the wing margin, the vein and an area at the wing joint are stained by Eosin Y. (G) Eosin Y penetrates the entire tissue after incubation of specimens at 60°C following incubation at 80°C and annealing. (H) Impermeability to Eosin Y at 25°C is restored when animals are cooled down to 0°C after incubation at 80°C. (I) In summary, two barriers – one temperature dependent (barrier 1) and one sensitive to chloroform (barrier 2) – prevent Eosin Y penetration into the wing blade. Barrier 2 components denature at 80°C. CHCl₃, chloroform.

high temperatures. Complete breakdown of both penetration barriers, in conclusion, occurs at 80°C. This effect cannot be reversed as Eosin Y is taken up by the entire surface after incubation of whiteflies at 60°C following chilling after 80°C incubation. In *D. melanogaster*, the situation seems to be simpler (Wang et al., 2016). Upon incubation in chloroform, Eosin Y stains the entire wing of *D. melanogaster*. Hence, lipid solvent application and temperature do not have an additive effect in this insect. A putative temperature-sensitive barrier in *D. melanogaster* does not play any role if the solvent-sensitive barrier is broken.

Chloroform and temperature have an additive effect on Eosin Y penetration in the bedbug cuticle

Eosin Y did not infiltrate the surface of *C. lectularius* first instar nymphs at temperatures below 65°C (Fig. 2). The first regions taking up Eosin Y at 65°C were the tips of the antennae. At 70°C, the entire antennae, the thorax, the posterior end of the abdomen and the tarsi of these animals became red. The whole animal was stained by Eosin Y at 75°C. However, at this temperature, redness of the leg joints was more intense compared with the other leg regions. Staining intensity of the legs was uniform at 80°C.

Washing first instar nymphs in chloroform before staining with Eosin Y led to dye uptake into the antennae, the thorax and the posterior region of the abdomen at 25°C, while the legs and a large abdominal area remained unstained (Fig. 2). Washing these animals with chloroform followed by their incubation at 60°C resulted in complete staining of the animal body, excluding the legs. Leg joints of chloroform-treated nymphs were stained at temperatures above 70°C. Uniform leg staining was observed after incubation at 75°C and did not intensify at 80°C. These observations indicate that for Eosin Y to penetrate into the bedbug cuticle, especially in the abdomen, two penetration barriers have to be trespassed. Re-incubation of bedbugs at 60°C after a cycle of incubation at 80°C and chilling resulted in complete Eosin Y uptake, while re-incubation at 25°C after the same initial incubation–chilling cycle

resulted in no staining (Fig. 2). These findings support our assumption of a double inward barrier in bedbug nymphs.

Bromophenol Blue and Methylene Blue behave like Eosin Y in penetration assays

To test whether the results obtained with Eosin Y are specific to this dye, we performed the same set of experiments described above using Bromophenol Blue or Methylene Blue. In principle, Bromophenol Blue and Methylene Blue mimicked the findings with Eosin Y. These results are shown in Figs S2 and S3.

Conclusions and outlook

Together, our experiments allow the distinction of regions of inward permeability conferred by two sub-barriers in the cuticle of *T. vaporariorum* and *C. lectularius*. What is the nature of these barriers? Our experiments addressed physico-chemical, i.e. material, rather than physiological (cell-based) properties of the cuticle. These properties nevertheless correspond to biological properties of the extracellular cuticle. Insensitivity of the barrier to relatively high temperatures between 40 and 60°C, at which most if not all proteins denature, and restorability together argue against an important role of cuticle proteins in constituting these barriers. Conceptually, we postulate that two distinct classes of Eosin Y-repellent, i.e. lipophilic, compounds are involved in inward barrier constitution in *T. vaporariorum* and *C. lectularius* (Figs 11 and 20). A fraction of free and solvent-soluble and high temperature-sensitive lipophilic compounds, probably CHCs, constitute one sub-barrier. The other sub-barrier is composed of a fraction of non-soluble lipophilic compounds that are sensitive to temperatures lower than those that modify the function of the first barrier. Lipophilic compounds, especially at the cuticle surface, have been repeatedly demonstrated to prevent dehydration in various insect species (Wigglesworth, 1971; Gibbs, 2002). Thus, the inward and outward barriers seem, at least concerning the CHCs, to rely on the same class of cuticular components. Thus,

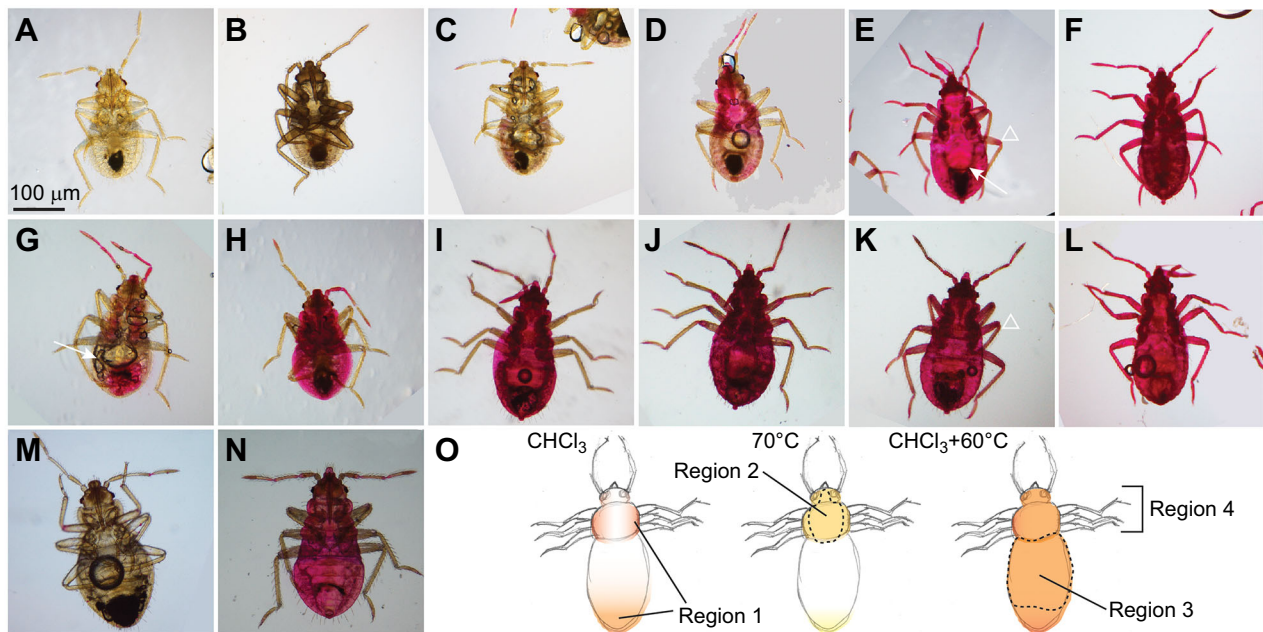


Fig. 2. Two cuticular barriers in *Cimex lectularius*. (A–L) Eosin Y staining of *C. lectularius* first instar nymphs at 25°C (A,G), 60°C (B,H), 65°C (C,I), 70°C (D,J), 75°C (E,K) and 80°C (F,L) alone (A–F) and after chloroform wash (G–L). (M,N) Cooling down nymphs to 0°C after incubation at 80°C restores impermeability to Eosin Y at 25°C (M), but not at 60°C (N). (O) Together, these experiments allow distinction of four regions of permeability.

the lipid-melting model for phase transition of surface lipids formulated by Ramsey for the outward barrier may also apply to the inward barrier.

Structurally, the double barrier does not have to necessarily be attributed to the envelope only. The pore canals, as potential sites of uncontrolled water flow, may also be equipped with material (CHCs or any other hydrophobic substance) to plug this route, at the same time preventing dye uptake. In this scenario, the two experimentally separable barriers may also be spatially distinct structures. Regardless, barrier properties are simpler in the model insect *D. melanogaster*, where no additive effects of two permeability barriers were observed. Detailed molecular and histological analyses of the whitefly and bedbug cuticles are needed to understand the bipartite barrier against penetration of hydrophilic molecules like Eosin Y, Bromophenol Blue and Methylene Blue. In theory, work on the inward barrier will also enhance our knowledge on the mode of action of hydrophobic molecules during cuticle penetration. The probable regionalised distribution of lipids and waxes would determine the preferred site of entry of this type of molecule at ambient temperature. Together, exploration of insect cuticle barrier properties may enable better understanding of the route of penetration used by contact insecticides that have to overcome the cuticle barrier in order to eliminate the insect during pest control.

Acknowledgements

We thank Ulrich Büsing from Nuetzlinge.de and Peter Katz from Katz Biotech AG for providing adult *T. vaporariorum*. We thank Klaus Reinhardt for bedbug nymphs.

Competing interests

The authors declare no competing or financial interests.

Author contributions

Y.W. and B.M. designed the experiments and they were performed by Y.W., R.G.C. and B.M. B.M. wrote the manuscript with contributions from Y.W. All authors approved the submitted manuscript.

Funding

This project was funded by the Deutsche Forschungsgemeinschaft (MO1714/7) and the Interfaculty Centre for Pharmacogenomics and Pharma Research (ICEPHA) graduate programme (project 5).

Data availability

Data are available from the Dryad Digital Repository (Wang et al., 2017): <http://dx.doi.org/10.5061/dryad.60nc3>.

Supplementary information

Supplementary information available online at <http://jeb.biologists.org/lookup/doi/10.1242/jeb.156679.supplemental>

References

- Darmanin, T. and Guittard, F.** (2015). Superhydrophobic and superoleophobic properties in nature. *Mater. Today* **18**, 273–285.
- Fischer, A. H., Jacobson, K. A., Rose, J. and Zeller, R.** (2008). Hematoxylin and eosin staining of tissue and cell sections. *CSH Protoc.* **2008**, pdb prot4986.
- Gibbs, A. G.** (1998). Water-proofing properties of cuticular lipids. *Am. Zool.* **38**, 471–482.
- Gibbs, A. G.** (2002). Lipid melting and cuticular permeability: new insights into an old problem. *J. Insect. Physiol.* **48**, 391–400.
- Gibbs, A. G.** (2011). Thermodynamics of cuticular transpiration. *J. Insect. Physiol.* **57**, 1066–1069.
- Gundersen, H., Leinaas, H. P. and Thaulow, C.** (2014). Surface structure and wetting characteristics of collembola cuticles. *PLoS ONE* **9**, e102961.
- Locke, M.** (1965). Permeability of insect cuticle to water and lipids. *Science* **147**, 295–298.
- Marconi, G. and Quintana, R.** (1998). Methylene blue dyeing of cellular nuclei during salpingoscopy, a new *in-vivo* method to evaluate vitality of tubal epithelium. *Hum. Reprod.* **13**, 3414–3417.
- Moussian, B.** (2010). Recent advances in understanding mechanisms of insect cuticle differentiation. *Insect. Biochem. Mol. Biol.* **40**, 363–375.
- Noble-Nesbitt, J.** (1970). Structural aspects of penetration through insect cuticles. *Pestic. Sci.* **1**, 204–208.
- Ramsay, J. A.** (1935). The evaporation of water from the cockroach. *J. Exp. Biol.* **12**, 373–383.
- Reinhardt, K., Naylor, R. and Siva-Jothy, M. T.** (2003). Reducing a cost of traumatic insemination: female bedbugs evolve a unique organ. *Proc. R. Soc. B Biol. Sci.* **270**, 2371–2375.
- Rourke, B. C. and Gibbs, A. G.** (1999). Effects of lipid phase transitions on cuticular permeability: model membrane and *in situ* studies. *J. Exp. Biol.* **202**, 3255–3262.
- Selman, G. G.** (1960). Certain aspects of bromophenol blue staining deduced from spot tests on filter-paper. *J. Chromatogr. A* **3**, 531–535.
- Sun, M., Liang, A., Watson, G. S., Watson, J. A., Zheng, Y., Ju, J. and Jiang, L.** (2012). Influence of cuticle nanostructuring on the wetting behaviour/states on cicada wings. *PLoS ONE* **7**, e35056.
- Wang, Y., Yu, Z., Zhang, J. and Moussian, B.** (2016). Regionalization of surface lipids in insects. *Proc. R. Soc. B Biol. Sci.* **283**, 20152994.
- Wang, Y., Carballo, R. G. and Moussian, B.** (2017). Data from: Double cuticle barrier in two global pests, the whitefly *Trialeurodes vaporariorum* and the bedbug *Cimex lectularius*. *Dryad Digital Repository*. <http://dx.doi.org/10.5061/dryad.60nc3>.
- Watson, G. S., Cribb, B. W. and Watson, J. A.** (2010). The role of micro/nano channel structuring in repelling water on cuticle arrays of the lacewing. *J. Struct. Biol.* **171**, 44–51.
- Wigglesworth, V. B.** (1971). Bound lipid in the tissues of mammal and insect: a new histochemical method. *J. Cell Sci.* **8**, 709–725.
- Wigglesworth, V. B.** (1975). Incorporation of lipid into the epicuticle of *Rhodnius* (Hemiptera). *J. Cell Sci.* **19**, 459–485.
- Wigglesworth, V. B.** (1986). Temperature and the transpiration of water through the insect cuticle. *Tissue Cell* **18**, 99–115.
- Wigglesworth, V. B.** (1990). The distribution, function and nature of “cuticulin” in the insect cuticle. *J. Insect Physiol.* **36**, 307–313.

Appendix 3: The ABC transporter Snu and the extracellular protein SnsI cooperate in the formation of the lipid-based inward and outward barrier in the skin of *Drosophila*.

Zuber, Renata; Norum, Michaela; Wang, Yiwen; Oehl, Kathrin; Gehring, Nicole; Accardi, Davide; Bartozsewski, Slawomir; Berger, Jürgen; Flotenmeyer, Matthias and Moussian, Bernard (2018). **The ABC transporter Snu and the extracellular protein SnsI cooperate in the formation of the lipid-based inward and outward barrier in the skin of *Drosophila*.** In: *Eur J Cell Biol.* 97(2), S. 90-101.DOI: 10.1016/j.ejcb.2017.12.003.



Research paper

The ABC transporter Snu and the extracellular protein Sns1 cooperate in the formation of the lipid-based inward and outward barrier in the skin of *Drosophila*



Renata Zuber^{a,1}, Michaela Norum^{b,1}, Yiwen Wang^b, Kathrin Oehl^b, Nicole Gehring^b, Davide Accardi^c, Slawomir Bartoszewski^d, Jürgen Berger^e, Matthias Flötenmeyer^e, Bernard Moussian^{a,f,*}

^a Applied Zoology, TU Dresden, Zellescher Weg 20b, 01217, Dresden, Germany

^b Interfaculty Institute for Cell Biology, Animal Genetics, Auf der Morgenstelle 15, 72076 Tübingen, Germany

^c Max-Planck Institute of Molecular Cell Biology and Genetics, Pfotenhauerstr. 108, 01307, Dresden, Germany

^d Rzeszow University, Department of Biochemistry and Cell Biology, ul. Zelwerowicza 4, 35-601 Rzeszów, Poland

^e Max-Planck Institute for Developmental Biology, Spemannstr. 35, 72076 Tübingen, Germany

^f iBV, Université Nice Sophia-Antipolis, Parc Valrose, 06108, Nice, France

A B S T R A C T

Lipids in extracellular matrices (ECM) contribute to barrier function and stability of epithelial tissues such as the pulmonary alveoli and the skin. In insects, skin waterproofness depends on the outermost layer of the extracellular cuticle termed envelope that contains cuticulin, an unidentified water-repellent complex molecule composed of proteins, lipids and catecholamines. Based on live-imaging analyses of fruit fly larvae, we find that initially envelope units are assembled within putative vesicles harbouring the ABC transporter Snu and the extracellular protein Sns1. In a second step, the content of these vesicles is distributed to cuticular lipid-transporting nanotubes named pore canals and to the cuticle surface in dependence of Snu function. Consistently, the surface of *snu* and *sns1* mutant larvae is depleted from lipids and cuticulin. By consequence, these animals suffer uncontrolled water loss and penetration of xenobiotics. Our data allude to a two-step model of envelope i.e. barrier formation. The proposed mechanism in principle parallels the events occurring during differentiation of the lipid-based ECM by keratinocytes in the vertebrate skin suggesting establishment of analogous mechanisms of skin barrier formation in vertebrates and invertebrates.

1. Introduction

Commonly, extracellular matrices (ECM) play essential roles in epithelial tissue function. Compared to proteins and sugars, lipids as constituents of ECMs have been studied only in few cases. In vertebrates, for instance, the outermost protective layer of the skin consists of a lipid-based ECM, the lamellar membrane, a network of lipids and proteins produced by keratinocytes (Koster, 2009; Nishifuji and Yoon, 2013). Mutations abrogating this matrix are associated with severe skin diseases in humans (Roberson and Bowcock, 2010; van Smeden et al., 2014). Another prominent example of a lipid-based ECM is the pulmonary surfactant that stabilises alveoli (Goerke, 1998). Failure to produce the surfactant provokes lethal lung diseases (Beers and Mulugeta, 2017). In insects, lipids are reported to cover the body

surface and to impregnate the non-cellular cuticle, which is assembled at the apical side of the epidermis (Moussian, 2010). Surface lipids, mostly alkanes and alkenes, are free, and have been considered to play an important role in dehydration and penetration protection (Gibbs, 1998; Gibbs, 2002; Wang et al., 2017; Wang et al., 2016). Integral lipids are immobilised within the cuticle through association with proteins and catecholamines. These complex molecules that besides of being key components of the waterproof barrier, also contribute to cuticle colour and stiffness, were named cuticulin by Sir Vincent Wigglesworth (Wigglesworth, 1933, 1990). In 1933, he described cuticulin as an “amber coloured material, more or less mixed with melanin” and “a fatty and waxy substance” that he refined almost 60 years later as “a compost of sclerotin (quinone-tanned protein) with lipid”. Presence of cuticulin is indicated when after removal of wax, sclerotin interacts

* Corresponding author at: iBV, Université Nice Sophia-Antipolis, Parc Valrose 06108 Nice, France.

E-mail address: bernard.moussian@unice.fr (B. Moussian).

¹ These authors contributed equally to the work and are co-first authors.

with silver ions in the argentaffin reaction in histological experiments. The molecular nature of cuticulin is, despite the long period of research, still enigmatic.

A major site of cuticulin accumulation is the outermost cuticle layer envelope. In *Drosophila melanogaster*, the envelope is constructed in three steps (Moussian, 2010; Moussian et al., 2006a). At the ultrastructural level, first, fragments of the envelope precursor consisting of two electron-dense sheets separated by an electron-lucid one are deposited into the extracellular space at the tips of irregular protrusions of the apical plasma membrane. Subsequently, these structures fuse to form a single layer covering the body of the developing embryo. Interestingly, fusion of envelope fragments at cell–cell contacts is the last step in this process (Fristrom and Liebrich, 1986). Next, when cuticle differentiation proceeds and the inner cuticle layers i.e. the epicuticle and the procuticle are formed, an electron-dense sheet intercalates into the electron-lucid sheet. The time point of this step of envelope maturation conceptually coincides with the time point of cuticulin deposition at the end of moulting in the kissing bug *Rhodnius prolixus* as observed by Wigglesworth (Wigglesworth, 1946). Transport and deposition of envelope material through the cuticle to the surface occurs via so called pore and wax canals, which are membranous tubes running from the apical surface of the epidermal cells to the surface of the cuticle. While delivery of lipids to target cells is well investigated (Chino et al., 1981; Palm et al., 2012), the underlying molecular mechanisms of lipid transport and integration into the cuticle or cuticulin formation are not understood.

In order to learn more about the mechanisms of lipid-based barrier construction, we conducted a screen for cuticle-deficient phenotypes caused by RNA interference (RNAi) in the late embryonic epidermis of *Drosophila melanogaster* that is mainly occupied with cuticle differentiation. Among others, we identified the ABC transporter CG9990 (Snustorr, Snu) and the extracellular protein CG2837 (Snustorr snarlik, Sns1) as essential factors involved in construction of the barrier against dehydration and penetration of water and xenobiotics. Based on our phenotypic analyses of *snu* and *sns1* we propose that Snu is involved in deposition of a yet uncharacterised, presumably lipidic material within the cuticle where it is immobilised by Sns1, which thus may constitute one of the protein components of Wigglesworth's cuticulin.

2. Materials & methods

2.1. Fly husbandry

For embryo and larva collection, flies were kept in cages on yeast apple juice agar plates. Embryos were staged according to the gut morphology and the time of development at 25 °C described in Hartenstein and Campos-Ortega (Hartenstein and Campos-Ortega, 1985) and dechorionated for three minutes in commercially available chlorine bleach diluted 1:1 in tap water. Homozygous or transheterozygous mutant embryos and larvae were manually collected in a population of progeny segregating a respective balancer chromosome expressing GFP (Dfd > YFP or Kr > GFP) and the mutation-bearing non-GFP chromosome. For techniques that require removal of the vitelline membrane the embryos were devitellinized by shaking in equal amounts of heptane and methanol (fixed embryos), or manually in PBS buffer (live embryos).

2.2. RNAi screen and Snu and Sns1 knockdown larvae

For the RNA interference (RNAi)-based screen for cuticle phenotypes, the Berkley *Drosophila* Genome Project (BDGP) *in situ* database was first searched for genes that are specifically expressed in the epidermis during mid to late stages of development when the cuticle is formed. Next, to analyse the function of a given factor during embryonic cuticle formation, flies harbouring the respective UAS-RNAi construct from the Vienna *Drosophila* RNAi Centre (VDRC) (Dietzl et al.,

2007) were crossed to flies expressing the epidermal Gal4-driver 69B-Gal4 and *dicer2* (UAS-*dicer2*) that has been reported to enhance RNAi efficiency. In total, 129 UAS-RNAi lines representing 75 candidate genes were tested. As a first indication for the importance of a factor for embryonic cuticle formation, embryonic lethality was assessed. When lethality of the offspring exceeded 30%, cuticle preparations of the lethal fraction were made following the protocol of Nüsslein-Volhard and Wieschaus (Nüsslein-Volhard et al., 1984) to analyse the phenotype. As controls for screen efficiency, RNAi silencing of *krotzkopf verkehrt* (*kkv*) and *knickkopf* (*knk*) (Moussian et al., 2005; Moussian et al., 2006b) was conducted. As a negative control flies harbouring the Gal4 driver were crossed to *w¹¹¹⁸* flies.

For further phenotypic analyses of *snu* (#107544 VDRC) and *sns1* (#104558 VDRC), flies with the respective UAS-RNAi construct were crossed to flies expressing both Gal4-drivers *da-Gal4* and *7063-Gal4* (maternal Gal4). Crosses were generally kept on yeast apple juice agar plates at 25 °C over night. *snu* RNAi L2/L3 knockdown larvae were additionally obtained by crossing *snu* UAS-RNAi flies with *hsp70-Gal4* (#2077, BDSC) flies. Gal4 expression by *hsp70-Gal4* is leaky in some epidermal cells; hence, to avoid heat shocking that may damage larvae, we developed a protocol taking advantage of the Gal4 leakiness. Larvae were kept at 18 °C until early L2 stage. Then they were transferred to 20 °C, 22 °C, 25 °C and 28 °C, respectively, to avoid heat-shock induction, and enhanced RNAi effect during L2/L3 transition in the leakage areas.

2.3. Molecular biology

Total mRNA was prepared from OrR wild-type stage 17 embryos (RNeasy Micro Kit, Qiagen). Total cDNA was prepared from the mRNA (Superscript III First-Strand Synthesis System, Invitrogen), which was used as a template for amplification of *snu* (Expand High Fidelity PCR System, Roche). Two alternative 5' primers, ATGGCGCCGAAGAAAG AGG and ATGCTGATATCAACTATTTCCAC, and one 3' primer, CCAACGCGGCTAGGATCTT were used for the amplification of three different isoforms. The products were ligated into the pCR2.1 TOPO vector (Invitrogen), which was used as a template for another PCR reaction with the same primer combinations. The product was ligated into the pCR8/GW/TOPO vector (Invitrogen). Sequencing of the purified vector DNA (Miniprep kit, Qiagen) confirmed the presence of *snu* isoforms A and B. Next, LR recombination was used to clone the cDNA into Gateway vector pTGW, which contains a UAS promoter and a GFP tag N-terminal to the insert. The vector was amplified in DH5alpha *E. coli* bacteria, purified (PerfectPrep Endofree Maxi Kit, 5Prime) and sent to Fly-Facility, (Clermont-Ferrand, France) for injection into *D. melanogaster* embryos.

For rescue studies using the UAS-GFP-SnuA construct, the UAS-GFP-SnuA insertion on the third chromosome was recombined on the chromosome harbouring the *snu^{Df(98E2)}* allele to obtain the UAS-GFP-SnuA, *snu^{Df(98E2)}* chromosome. Similarly, the insertions *tub-Gal4* or 69B-Gal4 were recombined to the *snu^{Df(98E2)}* carrying chromosome to obtain the *tub-Gal4/69B-Gal4, snu^{Df(98E2)}* chromosome. Flies with UAS-GFP-SnuA, *snu^{Df(98E2)}* were crossed to flies with *tub-Gal4/69B-Gal4, snu^{Df(98E2)}* in rescue experiments. To study Snu localisation, UAS-GFP-SnuA harbouring flies were crossed to *knk-Gal4* or *da-Gal4* flies and analysed by confocal microscopy.

In order to rescue the Sns1-deficient phenotype, flies with the deficiency uncovering the *sns1* gene *Df(2L)BSC182* were crossed to flies with *Twldl1 > Sns1-RFP* on the first chromosome. The *Twldl1 > Sns1-RFP* construct was synthesised by Genewiz at Sigma-Aldrich.

For quantitative real-time PCR (qPCR), cDNA from embryos and wing buds (dissected from mid-staged pupa) was prepared as described above. For amplification and detection, the Sybr-Green method was applied using an appropriate kit from Genaxxon (GreenMastermix) on a Roche LightCycler Nano as well as gene specific primers. As a reference, the expression of *rps20* was monitored. The $\Delta\Delta C_t$ values of *snu* and *sns1*

expression were calculated with the Roche inbuilt software.

2.4. Histology, microscopy and image preparation

For live imaging of fluorescence, larvae were anaesthetised with ether, mounted in glycerol or halocarbon 700 on a slide and covered by a coverslip. They were observed using Zeiss confocal microscopes (LSM 710, 780 or 880) equipped with a Plan-Apochromat 63X/1.4 Oil DIC M27 objective. The lasers and filters were: 405 nm/BP 420–480 nm and LP 605 nm, 488 nm/BP 420–480 and BP 495–550 nm, and 561 nm/BP 570–620 and LP645. The pinhole was set at 1 AU for each laser/filter combination. Specimens were scanned in a sequential mode. The Airy scan mode (Zeiss LSM 880) was employed to obtain the images of Fig. 8. Of note, we suppose that co-localisation of signals is imperfect in live imaging experiments. For the analysis of the emission of the auto-fluorescent substance, a Zeiss LSM 880 using the ZEN software was applied. Cuticle optical cross-section of live third instar *D. melanogaster* larvae was scanned with 405 nm laser light (Supplementary Fig. 7). Emission light was collected at wavelengths ranging of 415–691 nm in 8–9 nm sub-ranges creating 36 pictures. On a collective lambda mode picture (composed of superimposed 36 pictures) small round-shaped areas were designated and for each area a graph showing intensity – emission wavelength dependence was generated. All graphs from all areas were compared and divided into two groups. Graphs of these two groups showed a small shift of the maximum intensity. Two of the areas representing these two different types of graphs were taken as a reference and applied in a “linear unmixing” mode. The whole auto-fluorescent signal was divided into two parts corresponding to one of the graph type.

For analyses of melanisation, ready-to-hatch embryos were imaged by light microscopy (Nikon AZ100) and the grey scales of more than six head skeletons for each genotype were determined with the Adobe Photoshop CS3 software and statistically (*t*-test) analysed using the Microsoft Excel software. The mean value of 22 wild-type head skeletons was set as 100%.

For the determination of larval length and width, animals fixed in Hoyer's (30 g gum arabic, 50 ml distilled H₂O, 200 g chloral hydrate, 20 g glycerol, 1:1 diluted with lactic acid) were microscopied with a Nikon AZ100, imaged and analysed with the Nikon in-built software. Statistical analyses (*t*-test) were performed with Microsoft Excel software.

In penetration assays, live larvae were incubated in a 0,5% Eosin Y staining solution (Sigma-Aldrich) for 20 min at 25 °C and 40 °C, and subsequently washed with tap water before mounting for microscopy with a Leica Z4 using an unbuilt camera and Leica software. Wings of flies generated by the cross of *vg-Gal4* flies with UAS-*snu* or UAS-*snsI* flies were stained with Eosin Y following the same protocol. Bromophenol blue penetration was tested with 0,1% Bromophenol blue (Sigma-Aldrich) at room temperature for five minutes. Larvae were washed three times with tap water, and viewed on a Leica Z4 binocular.

For Sudan Black B staining, after dechoriation and mechanical removing of the vitelline membrane, wild-type, *snu* and *snsI* mutant stage 17 embryos were incubated with 100 µl Sudan Black B solution (0.5% in 70% ethanol, Sigma-Aldrich) over night at room temperature. Embryos were washed three times with 70% ethanol and incubated in 70% for six hours for destaining. Specimens were transferred to a glass slide, embedded in halocarbon oil and analysed by light microscopy.

For argentaffin detection, we modified a protocol published by Wigglesworth (Wigglesworth, 1985a, 1985b) for staining *D. melanogaster*. Modification was necessary because the original protocol includes the preparation of the insect by incubation in chloroform at 60 °C, a treatment that causes disintegration of the *D. melanogaster* larvae. Five to ten stage 17 embryos were freed manually from the egg case using needles after dechoriation in 50% bleach for 3 min. They were collected in 200 µl of 5% (w/v) AgNO₃. After collection, 800 µl of 2.5% (w/v) Tris base were added. Larvae were incubated in this solution for

one hour at 60 °C. Staining reaction was stopped with 1 ml of a 2.5% Thiosulphate solution. Stained larvae were analysed using a Nikon AZ100 microscope with a Nikon camera and NIS software.

For transmission electron microscopy (TEM), embryos and larvae were treated as described in (Moussian and Schwarz, 2010). A Philips CM-10 was used at 60 kV for data recording. For scanning electron microscopy (SEM), we applied a protocol published in Moussian 2006.

Figures were prepared using the Adobe Photoshop CS3 and Adobe Illustrator CS4 software without changing the initial settings of the microscope.

3. Results

In order to identify new factors of cuticle formation, we conducted a screen for cuticle defective phenotypes caused by RNAi-driven knock-down of transcripts that according to the modeENCODE and FlyExpress databases (Graveley et al., 2011; Kumar et al., 2011) are expressed in the late embryonic epidermis (see materials & methods).

3.1. *CG9990* and *CG2837* are essential for integument barrier construction

Living larvae systemically expressing hairpin RNA against *CG9990* or *CG2837* mRNA, are more translucent than wild-type larvae (Fig. 1A–C). When fixed with Hoyer's medium, these larvae shrink, without folding or wrinkling of the cuticle (Fig. 1D–F). *CG2837* knockdown larvae eventually hatch, but are flaccid and die around 10 min thereafter, whereas most and *CG9990* knockdown larvae fail to hatch. The tracheal system of these larvae is not gas-filled (Wang et al., 2015). Addition of halocarbon oil to newly hatched *CG2837* knockdown larvae rescues immediate lethality (Table 1). When manually freed from the egg case, larvae with reduced *CG9990* function are unable to maintain their body shape, flatten and dry out.

To analyse the effects of complete *snu* elimination, we characterised embryos and larvae homozygous mutant for the embryonic lethal deletion *Df(98E2)* that removes *CG9990* and the neighbouring gene *huntingtin* (*HTT*), which is dispensable for embryo development (Zhang et al., 2009). Indeed, expression of transgenic *CG9990* normalises the embryonic and larval *snu* mutant phenotype. Larvae homozygous mutant for *CG9990^{Df(98E2)}* are translucent and rapidly dehydrate, when manually freed from the egg case, overall paralleling the RNAi-induced phenotype (Fig. 1J).

To obtain a genetic stable constellation copying the *snsI* phenotype, we studied the embryonic phenotype caused by the deletion *Df(2L)BSC182* that removes *CG2837* and six neighbouring loci. Overall, phenotypes provoked by *Df(2L)BSC182* or systemic *CG2837^{RNAi}* (*daGal4/7063Gal4 > UASCG2837^{RNAi}*) are indistinguishable (Fig. 1K).

These results together suggest that *CG9990*- and *CG2837*-knockdown larvae suffer rapid water loss. The desiccation phenotype prompted us to name *CG9990 snustorr* (*snu*, Swedish for bone-dry), *CG2837 snustorr snarlik* (*snsI*, Swedish for *snu*-like).

3.2. *Snu* and *SnsI* contribute to the barrier against penetration

The cuticle is a bidirectional barrier, i.e. it does not only prevent water loss but also penetration of xenobiotics (Gibbs, 2011; Wang et al., 2016). To explore whether the cuticle of *snu* or *snsI* knockdown larvae is more permeable than the wild-type cuticle, we immersed these larvae in Eosin Y. Wild-type larvae remain unstained after incubation in Eosin Y at room temperature and at 40 °C. They take up Eosin Y at 55 °C. Reduction of *Snu* and *SnsI* function causes a dramatic uptake of Eosin Y through the integument already at 25 °C or 40 °C, respectively (Fig. 2A–C). Applying this protocol, we also tested permeability of the wing cuticle in wild-type flies and flies expressing hpRNA against *snu* or *snsI* transcripts in the wing (Fig. 2E–G). Of note, as detected by quantitative PCR (qPCR), both genes are expressed in wing buds during pupal development ($\Delta\Delta Ct$ against *rps20* expression: *snu*: $-2.49 + / -$

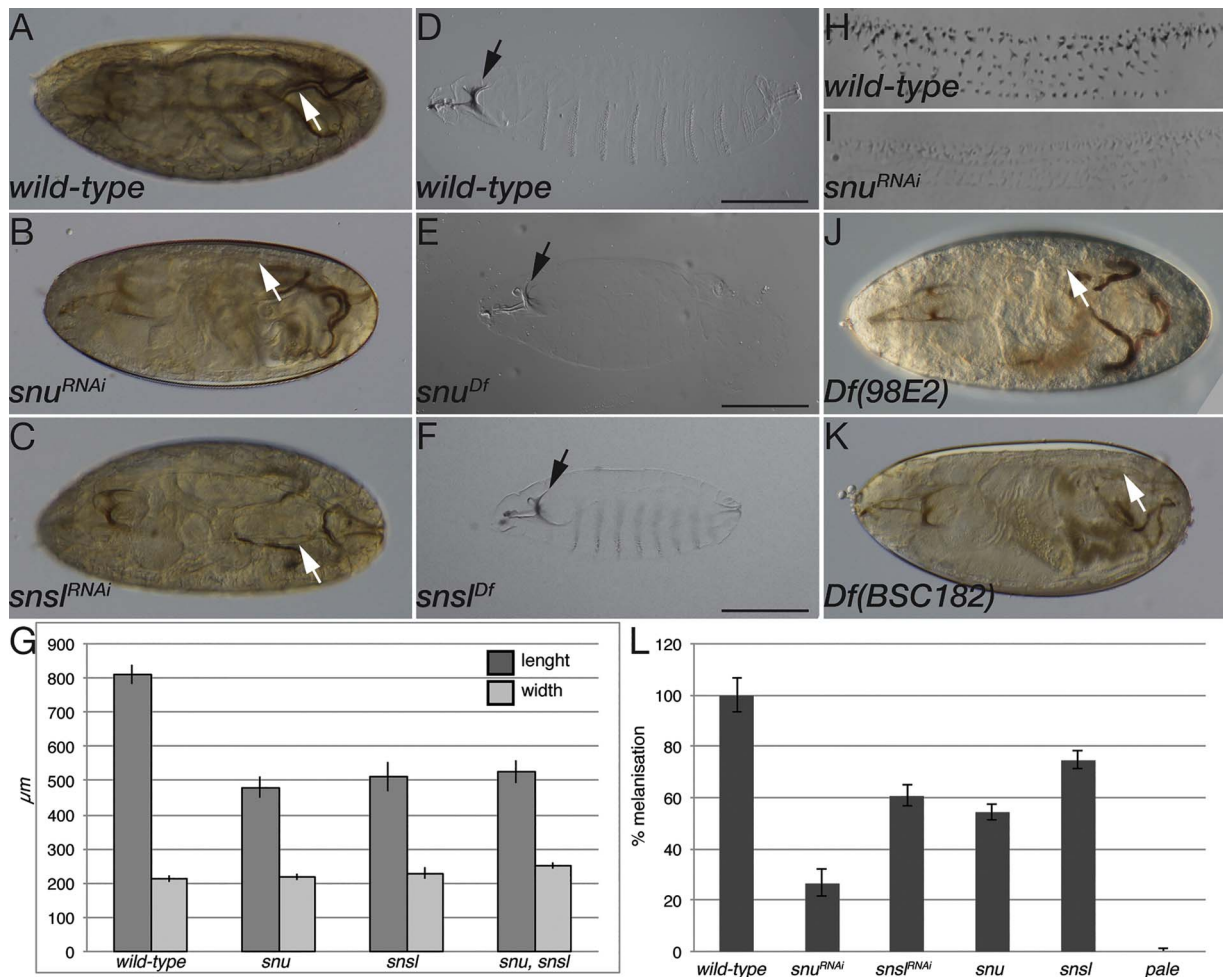


Fig. 1. Phenotype of larvae with reduced or eliminated *CG9990/snu* and *CG2837/snsl* expression.

At the end of embryogenesis, the larva ready to hatch is opaque, the inner organs are faintly visible; its tracheal system is filled with gas (A, white arrow). Reduction of *snu* or *snsl* expression provokes a fully transparent appearance. The outline of the inner organs of these animals is clearly visible. Their tracheal system is not filled with gas (B,C, white arrows). Cuticle preparations of wild-type (D) and *snu^{Df}* (E) or *snsl^{Df}* (F) mutant larvae reveal that the cuticle of *snu* and *snsl* larvae retracts. By consequence, the larvae are shorter (G). Data were obtained from 21 wild-type, 13 *snu^{Df(98E2)}*, 17 *snsl^{BSC182}* and 10 *snsl^{BSC182, snu^{Df(98E2)}}* animals. The differences from wild-type data are statistically significant with the *p*-values of 2,00658E-23, 7,35369E-26 and 5,68513E-18, respectively.

In particular in larvae with reduced *snu* expression, the head skeleton (black arrows) and the ventral denticles (shown here for the 4th abdominal segment) are paler (D-F, H,I). Live *snu^{Df}* (J) or *snsl^{Df}* (K) mutant larvae resemble those with reduced *snu* or *snsl* expression. Full melanisation of the head skeleton requires Snu, Snsl and Pale (L) Data were obtained from 22 wild-type, 13 *snu^{Df(98E2)}*, 15 *snu^{RNAi}*, 19 *snsl^{BSC182}*, 16 *snsl^{RNAi}* and 6 *pale* animals. The values for the larvae with deficient or reduced *snu*, *snsl* and *pale* function are in a *t*-test significantly different from the wild-type values with the *p*-value of 2.42674E-05, 1.5319E-09, 0.002035566, 4.59378E-05 and 3.37858E-08, respectively. Anterior is to the left, dorsal is to the top in A-F, J and K.

Table 1
Snsl prevents desiccation.

	wild-type	L370-Gal4xUASsnsl ^{RNAi}
without oil	> 2 h (n = 13)	12 min +/- 1.9 (n = 10)
with oil	> 2 h (n = 11)	> 2 h (n = 11)

In a simple desiccation test, wild-type and *snsl* knock-down larvae after hatching were either submerged in halocarbon oil or not. On air, *snsl* knock-down larvae died within 12 min, while wild-type larvae were alive during the 2 h of experiment. Submersion of *snsl* knock-down larvae in halocarbon oil prolonged lifetime.

0.19; $\partial\partial\text{Ct } snsl: -10.82 \pm 0.07$, see Materials and Methods). Wild-type wings do not take up Eosin Y at 25 °C. At 50 °C, by contrast, two areas in the posterior edge of the wings become red. Wings with reduced *snu* activity are impermeable to Eosin Y at 25 °C, whereas the entire wing blade is stained by Eosin Y at 50 °C. Reduction of *snsl* expression in wings does not interfere with Eosin Y uptake. Together, these findings demonstrate that *snu* and *snsl* are needed for inward barrier construction in the larval cuticle. In the wing cuticle, in contrast

to Snu the function of Snsl seems to be dispensable. Thus, different types of cuticles have different requirements for Snu and Snsl.

3.3. Cuticle envelope structure requires Snu and Snsl function

The envelope, the outermost cuticle layer, is considered as the water impermeable barrier in insects. For a detailed analysis of Snu and Snsl function, we studied the cuticle ultrastructure of respective mutant larvae by transmission electron microscopy (TEM). The wild-type larval cuticle consists of three composite horizontal layers (Fig. 3A) (Moussian, 2010). The outermost envelope has five alternating electron-dense and electron-lucid sublayers. Underneath lies the bipartite epicuticle. The innermost procuticle is a stack of helicoidally arranged sheets of parallel running chitin microfibrils (lamina). The envelope of *snu^{Df(98E2)}* mutant larvae is reduced with only two electron-dense sublayers and occasionally breaks open (Fig. 3B). Unusual electron-dense material is found at the cuticle surface of these larvae. This material was observed by scanning electron microscopy (SEM), as well (Fig. 3D,E). The *epi*- and procuticle, by contrast, appear to be normal in

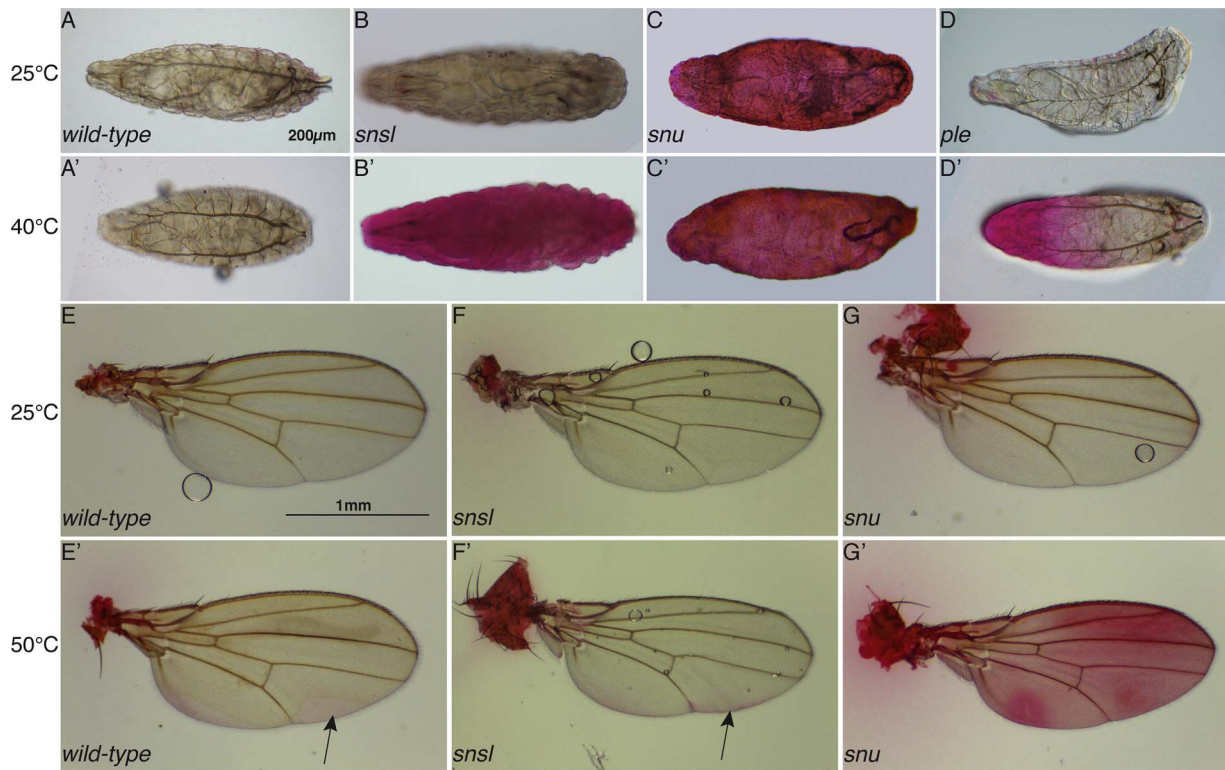


Fig. 2. Snu and Sns1 are needed for inward barrier function.

The integumental cuticle of living wild-type larvae before hatching is impermeable to Eosin Y at 25 °C and 40 °C (A,A'). The cuticle of *sns1* mutant larvae becomes permeable to Eosin Y at 40 °C (B,B'), whilst *snu* mutant larvae take up Eosin Y already at 25 °C (C,C'). Larvae mutant for *ple* show Eosin Y leakage in the anterior body part at 40 °C (D,D').

The wings of wild-type flies and flies with down-regulated *sns1* expression in the wings stain with Eosin Y at 50 °C in the two areas of the posterior part (E-F', arrows). The whole wings of the flies with down-regulated Snu activity in the wings are stained at 50 °C (G,G').

A-D' Dorsal view, anterior to the left. E-G' Anterior to the top.

these larvae. In addition to the aberrant envelope and despite their normal ultrastructure, the procuticle detaches from the epicuticle in the cuticle at apodemes (muscle attachment sites) of *snu* deficient larvae (Fig. 3F,G). The ultrastructure of the envelope of *sns1^{BSC182}* mutant appears to be normal. However, unusual electron-dense material is present at the surface of these animals (Fig. 3C).

In our experience, after excitation with 405 nm violet light, the surface of the *D. melanogaster* L1 larva emits a distinct autofluorescent signal at a broad range of 420–620 nm with the maximum peak around 475 nm (Fig. 4A-F). Further spectral analyses revealed a slight shift between the emission maxima at the upper and lower half of the fluorescing signal. This indicates that at least two materials with distinct optical properties form adjacent layers that constitute the surface of the *D. melanogaster* larva (Fig. 4H). At later larval stages additional dot-like structures (hereafter named 405-dots) are detected underneath the surface autofluorescence. These dots localise to the tips of filigree membrane protrusions, probably pore canals, visualised by CD8-RFP (Fig. 4, S1).

When excited with this light, the surfaces of living first instar larvae suffering *snu* or *sns1* elimination display only a very faint autofluorescence (Fig. 4B,C). Thus, presence of the autofluorescing layer in *D. melanogaster* larvae depends on Snu and Sns1 function. Our ultrastructural and fluorescence microscopy analyses together indicate that the surface autofluorescence depends on an intact envelope. Overall, we conclude that Snu and Sns1 are involved in envelope construction.

3.4. Envelope structure does not depend on melanisation or on di-tyrosine formation

In *snu^{Df(98E2)}* larvae, denticles and the head skeleton are barely melanised (Fig. 1D–E, H,I). To tackle the question whether the function

of Snu might depend on melanisation, we analysed 405nm-excited surface auto-fluorescence of larvae mutant for *pale* (*ple¹*) that codes for the first enzyme of the melanisation pathway. The surface auto-fluorescence of these larvae is not reduced compared to the signal in wild-type larvae (Fig. 4D). This finding suggests that melanisation is not needed for envelope integrity. This is consistent with the finding that the envelope ultrastructure of embryos mutant for *Ddc* encoding the second enzyme of the melanisation pathway is normal (Moussian et al., 2006a). However, permeability experiments showed that the cuticle of *ple* mutants is permeable to Eosin Y at a level comparable to the cuticle of *snu* mutant embryos (Fig. 2D,D'). This shows that either the disorders of the *ple¹* envelope are not detectable by confocal or electron microscopy, or there are two parallel mechanisms implementing cuticle impermeability.

Previously, by analysing the phenotype of δ -aminolevulinatase (*alas*) mutant larvae, we had shown that a heme-dependent pathway is needed to prevent sudden water loss in the *D. melanogaster* first instar larva probably by introducing di-tyrosine bounds into the cuticle (Shaik et al., 2012). We had reported that the envelope of *alas* deficient 1st instar larvae looked normal. Here, we tested, however, whether the surface autofluorescence in *alas* mutant larvae is intact (Fig. 4E). When excited with a 405 nm laser light source, the surface autofluorescence of these larvae appears to be normal. Thus, the heme biosynthesis pathway does not seem to contribute to the formation of the envelope as a waterproof barrier.

3.5. Snu and Sns1 are needed for cuticulin formation

According to Sir V. Wigglesworth the catecholamine-protein-lipid complex cuticulin contributes to cuticle waterproofness, tanning and stiffness (Wigglesworth, 1933, 1990). Concerning the pale cuticle, the

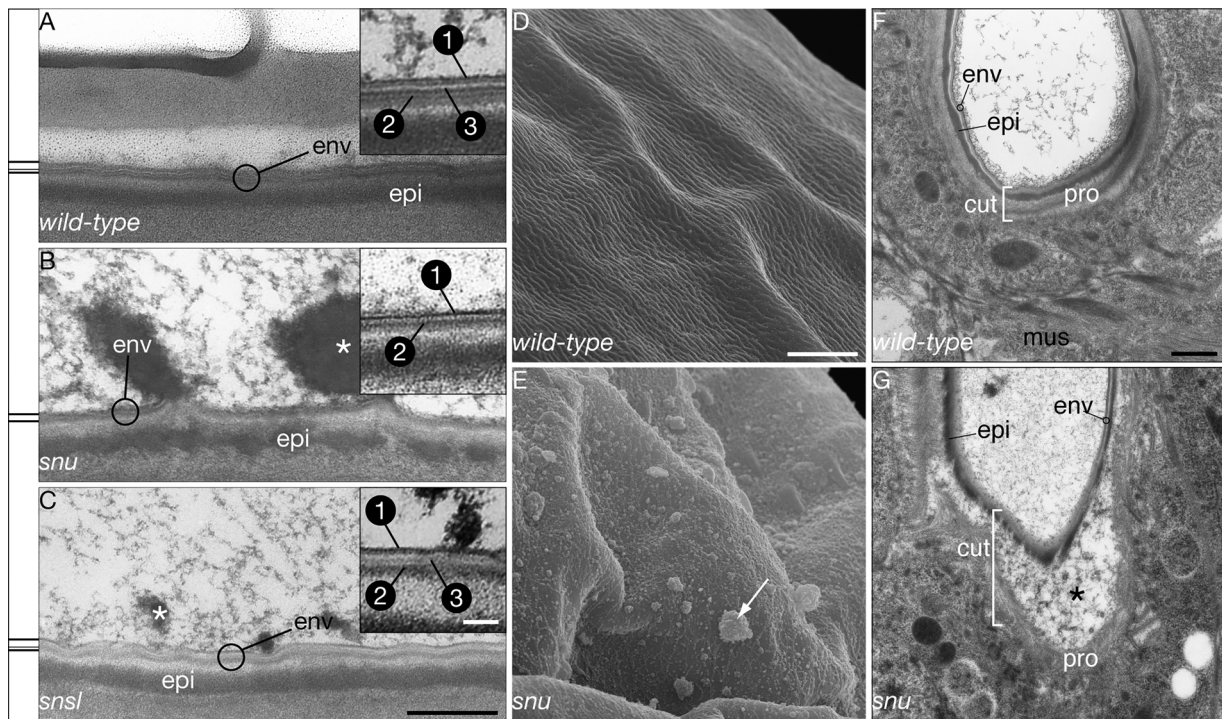


Fig. 3. Snu and Sns1 are needed for envelope construction.

In transmission electron-micrographs, the envelope (env) of the integumental cuticle of wild-type first instar larva consists of three electron-dense and two electron-lucid alternating sheets above the epicuticle (epi) (A). In *snu* mutant larvae, the envelope is composed of two electron-dense sheets separated by one electron-lucid one (B). Electron-dense material protrudes from the surface of these animals (*). The envelope of *sns1* mutant larvae appears to be normal (C). However, numerous electron-dense amorphous aggregates are found at the surface of these larvae (*). The wild-type first instar larval surface as visualised by scanning electron microscopy forms minute ridges (D). By contrast, the surface of *snu* mutant first instar larvae is covered by irregular aggregates (arrow, E).

At apodemes, as shown by transmission electron microscopy, the cuticle (cut) of the wild-type larva forms folds at muscle (mus) retraction (F). At these sites, the procuticle (pro) of *snu* mutant larvae detaches from the epicuticle (epi) when muscles retract (G).

Scale bars: A–C shown in A 500 nm; D and E shown in D 20 μ m, F and G shown in F 500 nm.

desiccation problem and the ultrastructural defects of the envelope, it is well possible that cuticulin integrity is affected in *snu* and *sns1* mutant larvae. Cuticulin, the molecular nature of which is yet unknown, can be visualised by the so-called argentaffin staining (see materials and methods). In wild-type larvae, silver grains precipitate at the surface of the cuticle (Fig. 5A). In *snu*^{Df(98E2)} mutant larvae and larvae with reduced Sns1 function, visibly less silver precipitates at the surface (Fig. 5B,C).

We also sought to visualise cuticular lipids using Sudan black staining followed by light microscopy (Fig. 5D–F). In wild-type and *sns1* mutant ready-to-hatch larvae, Sudan black stains the integument. By contrast, the integument of *snu* mutant larvae is unstained after incubation with Sudan black. Thus, in wild-type and *sns1* mutant larvae, integument lipids are present, while the amounts of lipids are reduced in the integument of *snu* mutant larvae.

Together, we conclude that Snu and Sns1 are needed for cuticulin production.

3.6. Snu codes for ABC transporters localised at the apical plasma membrane

To study the molecular and cellular function of Snu, we first analysed its protein sequence. The *snu* locus codes for six predicted isoforms of a half-type ABC transporter, the longest one, isoform A, harbouring 808 amino acids (Fig. S1). Standard homology searches reveal that all isoforms contain an ATP binding domain at the N-terminal half and a membrane-spanning region containing six (PSORTII and CCTOP) or seven (SMART) transmembrane helices within the C-terminal half of the protein (flybase.org). The C-terminus is predicted to have an ER retention signal that upon interaction with a putative partner may be

masked allowing the protein to continue travelling through the secretory pathway. Interestingly, none of the isoforms has a canonical N-terminal signal peptide. Snu-related sequences with the same domain composition are present in most arthropods suggesting that Snu function is conserved in this taxon (Fig. S1).

To verify the subcellular localisation of Snu, we generated an N-terminal GFP tagged version of Snu isoform A (GFP-SnuA) that is able to normalise the *snu* mutant phenotype (Fig. S2 and S3 1A–C). At larval stages GFP-SnuA localises to the apical surface of epidermal cells of living larvae. Some GFP-SnuA dots are detected within the cell, possibly marking transporting vesicles. Hence, Snu is an ABC transporter that exerts its role in the cell and/or vesicle membrane.

3.7. Sns1 localises to the tips of putative pore canals

What is the molecular and cellular role of Sns1? According to our sequence analyses, Sns1 is a secreted protein with an N-terminal signal peptide (Fig. S5). To verify the subcellular localisation of the Sns1 protein, we generated a C-terminal RFP-tagged version of Sns1 that is expressed under the control of an epidermal promoter (*twllm*, see materials and methods). Expression of Sns1-RFP protein in *sns1* deficient embryos restores the autofluorescent surface layer excited with a 405 nm laser and cuticular impermeability (Fig. S3 2A–C'). The signal of Sns1-RFP is rather weak and visible only in the epidermal cell at early larval stages (Fig. 6A), but well discernable at the third larval stage. In third instar larvae, Sns1-RFP is present in the cytoplasm and the cuticle. Here, it largely co-localises with the 405-dots underneath the envelope (Fig. 6B–D). Interestingly, the Sns1-RFP and 405-dots signals are comparably strong in epidermal hair structures (Fig. 6F–G'). We assume that the dots composed of Sns1-RFP and the blue fluorescing material

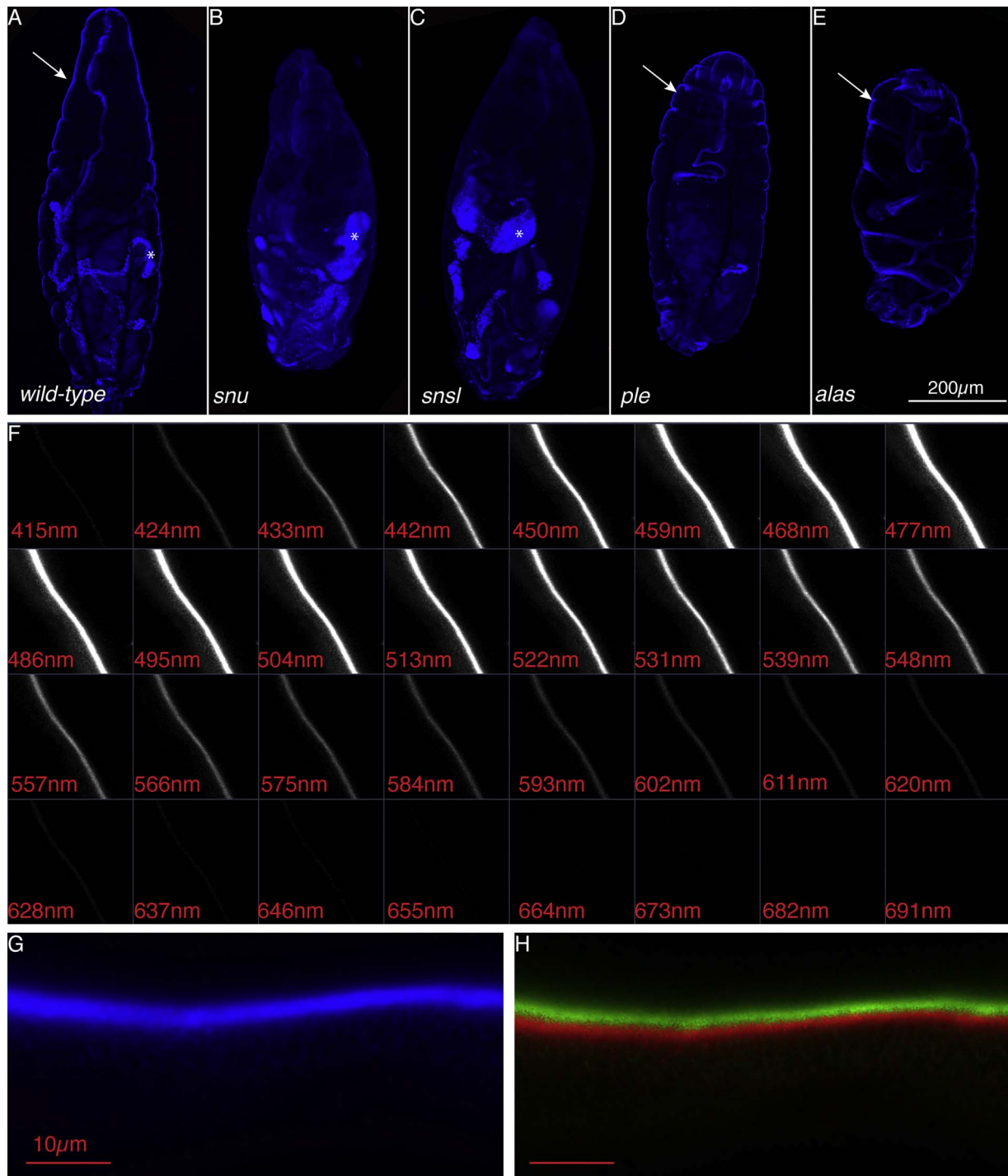


Fig. 4. The larval envelope that fluoresces in a wide range of wavelengths is depleted in *snu* and *snsl* mutant larvae.

When exposed to 405 nm light, the cuticle of the living wild-type *Drosophila* larvae before hatching emits a fluorescent signal (A). The cuticle of weakly melanised, permeable *snsl* and *snu* mutants does not emit this autofluorescent signal (B,C). Signal emission is normal in the cuticles of unmelanized *ple* (D) and *alas* mutants (E). Analysis of the emission spectrum of the surface autofluorescent light (lambda mode) of the cuticle of living third instar larvae shows a broad range of emission between the boundaries of 424 and 620 nm (F). The linear unmixing function reveals two potentially different substances in the autofluorescent region (G): the upper one is marked by green, and the lower part is marked by red (H).

underneath the envelope are the tips of the putative pore canals running from the cell surface to the surface of the cuticle. To test this assumption, we analysed the localisation of these dots in third instar larvae expressing the membrane-inserted protein CD8-GFP that like CD8-RFP, albeit weaker, marks thin vertical lines in the cuticle presumably representing the pore canals. *Snsl*-RFP and the 405-dots contact the tips of CD8-GFP marked vertical lines supporting the notion that the *Snsl*-RFP/405-dots are at the ends of the putative pore canals.

3.8. Localisation of *Snsl* in the cuticle depends on cell-autonomous *Snu* activity

The similar cuticle permeability problems associated with eliminated or reduced *Snu* and *Snsl* function argue that these proteins might collaborate or even interact with each other during envelope formation. Arguing that collaboration or interaction in the same process may necessitate co-localisation, we first tested whether the cytoplasmic

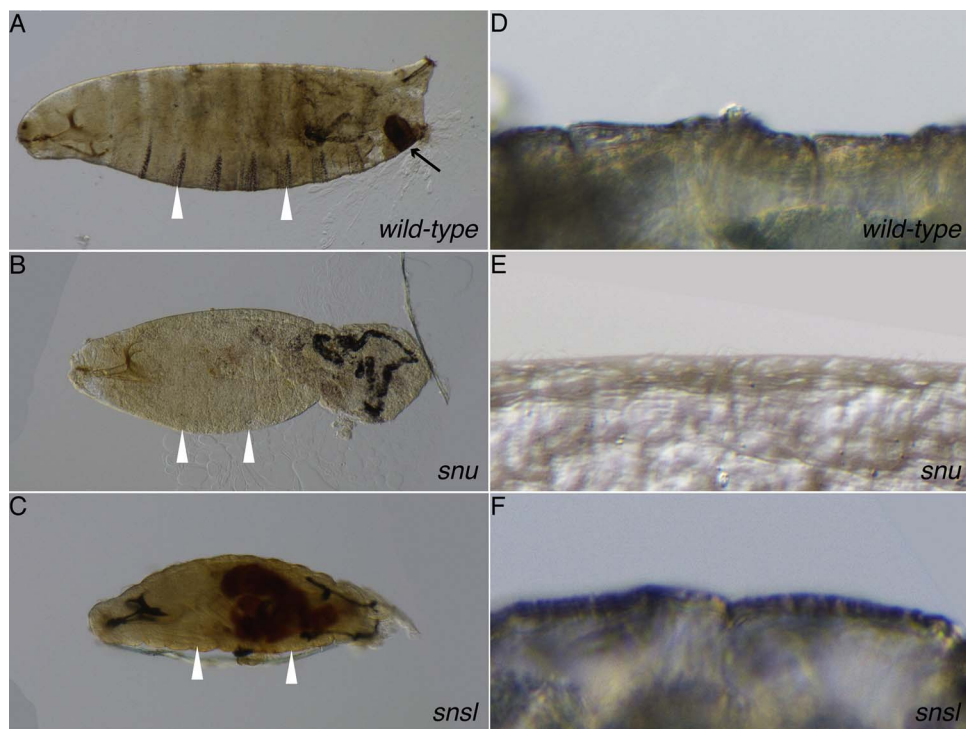


Fig. 5. Cuticulin deposition depends on Snu and Sns1. Silver grains precipitate predominantly at the surface of the anal pads of wild-type first instar larvae following our argentaffin staining protocol based on Wiggelsworth's protocol (A). Silver grains fail to recognise the surface of the anal pads of *snu* (B) or *sns1* (C) mutant first instar larvae. Sudan black marks the surface of wild-type first instar larvae (D). The surface of *snu* mutant first instar larvae is not stained by Sudan black (E), whilst the surface of respective *sns1* mutant larvae is (F).

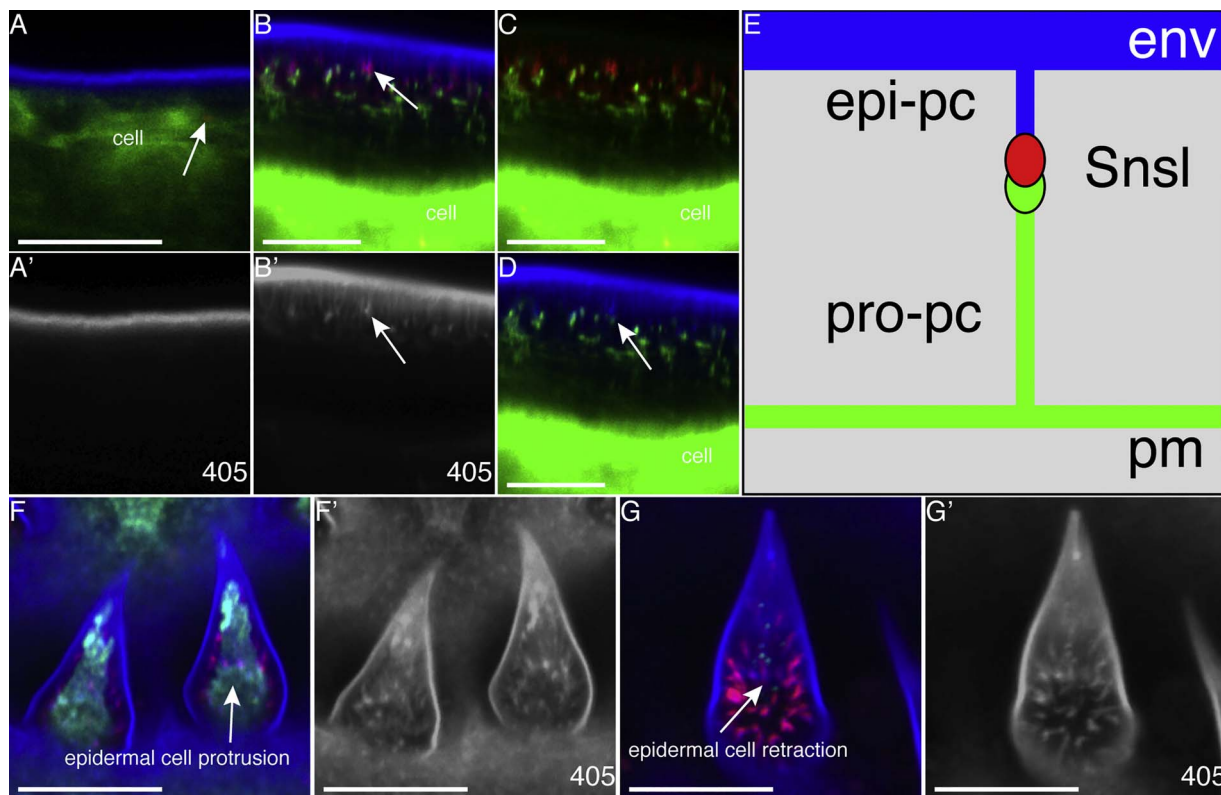


Fig. 6. Sns1 localises to putative pore canals. In living first instar larvae, the Sns1-RFP protein (red, arrow) is visible as single dots in the epidermal cells that are marked in green. No red signal is detectable in the integumental cuticle in or beneath the 405-signal of the envelope in first instar larvae (A,A'). Sns1-RFP is visible in the cuticle of late third instar larvae, where it largely overlaps with the 405-dots (B,B') and the tips of filigree membrane protrusions marked with CD8-GFP (B-D, arrows). Schematically, the epicuticular putative pore canals (*epi-pc*) are connected to the procuticular putative pore canals (*pro-pc*) through Sns1 (E). These structures are visualised clearer by the expression of CD8-RFP in the epidermis (Fig. S1). The epidermis (CD8-GFP, green, arrow) is present also in the middle of cuticular hairs of young third instar larvae (F,F') and retracts with time (G,G'), when the distance between the cuticular envelope (F',G') and the apical surface of epidermal cells increases. Sns1-RFP largely co-localises with autofluorescing (blue) canal-like structures of hairs that appear to connect the green epidermal cell with the envelope. Scale bar: 10 μm.

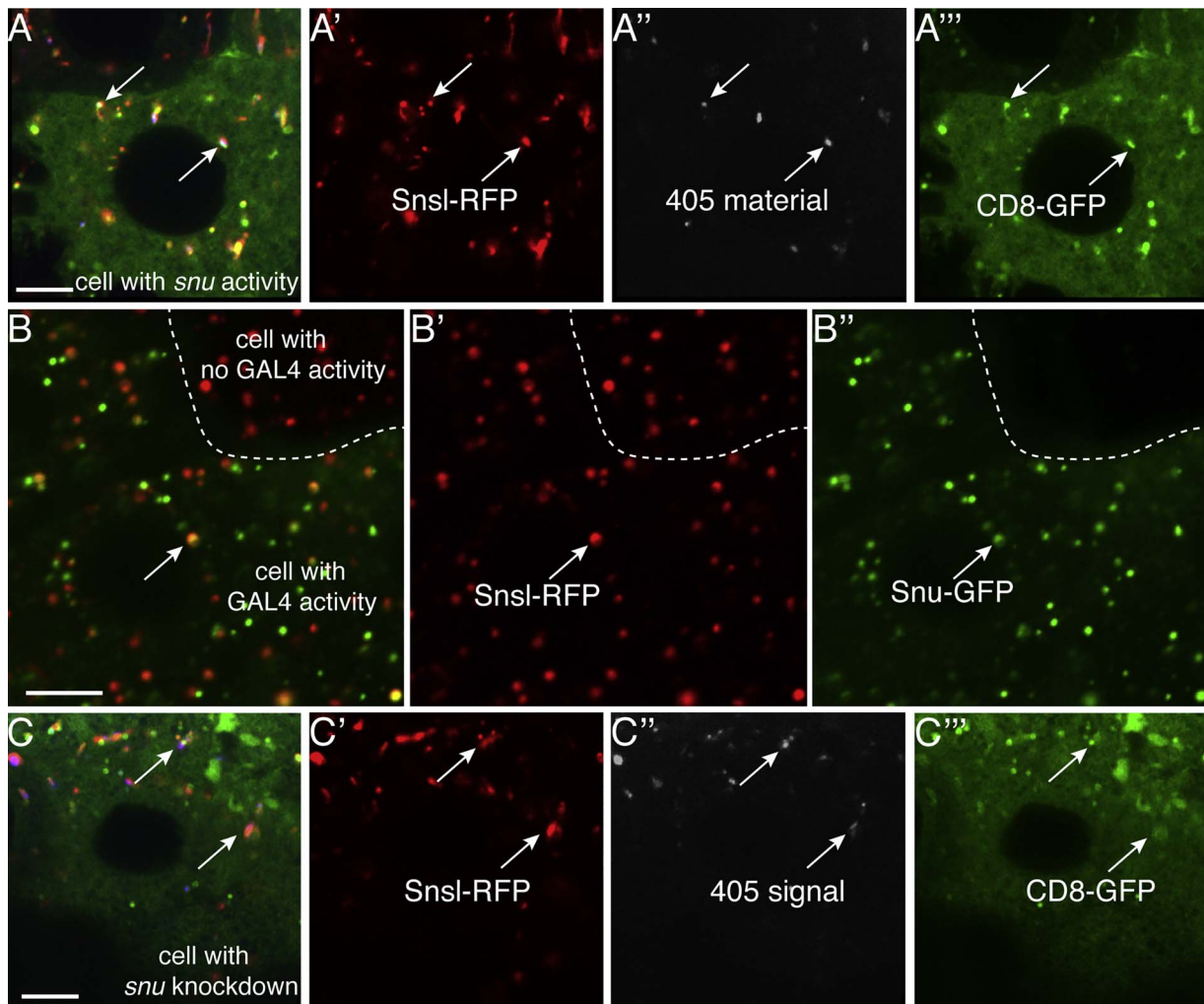


Fig. 7. Co-localisation of GFP-Snu, Sns1-RFP and 405-dots precursors in putative secretory vesicles. In the epidermal cells of wild-type living second instar moulting larvae, Sns1-RFP (red) and the 405-dot precursors (blue) are detected in the same structures (A–A'''), arrows). These structures are also marked by membranous CD8-GFP (green) indicating they are transport vesicles. In the epidermal cells of wild-type second instar moulting larvae, Sns1-RFP (red) largely co-localises with GFP-Snu (green) in the same putative vesicles (B–B'''), arrows). The white triangle points to a Snu-GFP-signal that is devoid of Sns1-RFP. The Gal4 driver used in this experiment has a mosaic expression. In the cells with down-regulated *snu* expression (C–C'''), 405-dots and red Sns1-RFP still largely co-localise in the membranous structures (arrows) indicating that Snu is not required for the vesicle loading process.

localisations of Snu and Sns1 coincide in live larvae. We observed that GFP-Snu and Sns1-RFP largely co-localise in the same dot-like structures within the epidermal cell, probably representing secretory vesicles (Fig. 7B–B'''). These structures also contain fluorescing material when excited with the 405 nm laser (Fig. 7A–A'''). The 405-dots and Sns1-RFP are found in the same structures when Snu expression is reduced by RNAi (Fig. 7C–C'''). Thus, GFP-Snu, Sns1-RFP and the 405 material are present in the same cytoplasmic structures. The presence of the 405 material and Sns1-RFP in these vesicles is independent of Snu function.

We next tested whether the extracellular localisation of Sns1-RFP depends on Snu function in larvae mosaic for Snu activity (Fig. 8). In cell clones with reduced Snu function, Sns1-RFP localises in the presumed procuticle. The Sns1-RFP signal in these cells largely overlaps with the ectopic 405-signal. Thus, correct delivery of Sns1 and of the 405-dots is dependent on full Snu function.

4. Discussion

Sir Wigglesworth proposed in 1933 that the catecholamine-lipid-protein complex cuticulin is a key factor in cuticular transpiration control in *Rhodnius prolixus* (Wigglesworth, 1933, 1990). After more than 80 years, the molecular composition of cuticulin is, however, still

elusive. In the present work, we report on the identification of three factors that we propose to be involved in cuticulin formation in the fruit fly *Drosophila melanogaster*.

4.1. Course of envelope construction

The cuticle envelope is a thin composite structure. It is composed of five alternating electron dense and electron lucid sheets (Moussian et al., 2006a). The *D. melanogaster* larval envelope is produced and assembled during embryogenesis sequentially (Moussian et al., 2006a). Fragments of envelope precursors with two electron-dense layers framing an electron-lucid layer are deposited into the extracellular space. They eventually fuse together forming a continuous sheet. An electron-dense layer intercalates within the electron-lucid layer and the envelope matures. Extensive protrusions of the apical plasma membrane called pore canals are reported to be the routes of surface i.e. envelope material delivery (Locke, 1961). In this work, we show that the surface of *D. melanogaster* larvae fluoresces when excited with a 405 nm light source. During cuticle formation, dots fluorescing upon illumination with this light source are detected within the epidermal cell and in the forming cuticle. Some of these dots also localise to the tips of the membranous structures that we suspect are pore canals (405-

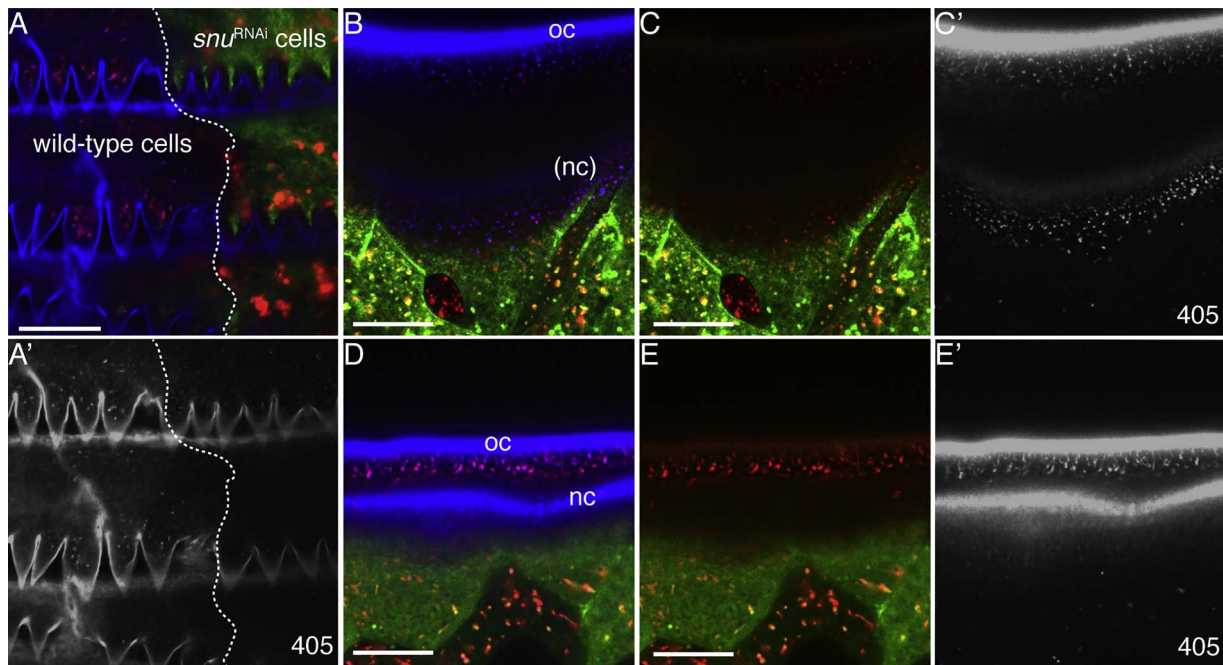


Fig. 8. Sns1 localisation depends on Snu function.

As observed in tangential optical sections of the integument of the moulting third instar larvae, in the epidermal clones with RNAi-induced *snu* expression reduction (marked with GFP, green) the autofluorescence signal (blue) is weaker (A,A'). The Sns1-RFP signal (red), which largely overlaps with the 405-dots in the pore canals in the extracellular space in wild-type clones, is intracellular in clones with reduced *snu* expression. In sagittal optical sections at higher magnification, below the very faint envelope of newly formed *snu*-deficient third instar larval cuticle (nc), 405-dots accumulate in the lower cuticular layers above the epidermal cells and largely co-localised with the Sns1-RFP signal that is discernable at this magnification (B-C'). The old cuticle (oc) established before the onset of RNAi is intact. In the extracellular space of respective control larvae accumulation of 405-dots and Sns1-RFP signal does not occur (D-E'). Scale bars: 10 μ m

dots). We reckon that 405-dots are components that are transported via these putative pore canals and are incorporated at the surface of the larvae constituting the envelope. Persistent localisation of this signal at the tips of the putative pore canals also indicates that a second population of this material additionally represents constituents of these membranes. Possibly, according to histological data of Wigglesworth localising polyphenols to the tips of pore canals, the 405 signal may be emitted by these types of molecules (Wigglesworth, 1988, 1990). The detailed relationship of polyphenols, the 405-dots and the ultrastructure of the envelope and the putative pore canals remains to be investigated.

4.2. *Snu* and *Sns1* are needed for envelope construction and function

Reduction or elimination of *snu* expression results in rapid water loss, uncontrolled uptake of external dyes and death of the larvae. As shown by electron microscopy, these larvae have a thin and depleted envelope. Thus, Snu is not needed for the first step of envelope formation. Depletion of the envelope is also recognisable with the fluorescence microscope. The surface, 405nm-excited fluorescence observed in wild-type larvae is lost in animals with reduced or eliminated Snu function. Instead, dotted 405 signal is detected within the procuticle and occasionally in the cell in these animals. At the ultrastructural level, we observe that an electron-dense sublayer, possibly the intercalated one, is missing. Furthermore, the integument of *snu* mutant larvae remains unstained after incubation with the lipid-marking dye Sudan black. Additionally, in argentaffin staining assays, the surface of *snu* mutant larvae fails to be marked with silver grains. These results indicate that lipophilic components in or at the cuticle are depleted when Snu is dysfunctional. The assumed orthologues of Snu in *Tribolium castaneum*, TcABCH-9C, and *Locusta migratoria*, LmABCH-9C have consistently been reported in lipid-staining experiments to be needed for the presence of lipids at the surface of the larvae or nymphs, which presumably are in turn required for desiccation resistance (Broehan

et al., 2013; Yu et al., 2017). We conclude that the ABC transporter Snu is needed to establish the envelope as a water-resistance barrier by mediating the incorporation of the 405-dots and lipophilic components into this layer.

A similar, albeit weaker larval phenotype is caused by reduction or elimination of *sns1* expression. These larvae are able to hatch after embryogenesis and die as first instar larvae that massively lose water. Dye penetration into these larvae occurs at higher temperatures than into *snu* deficient larvae, the cuticle of wings with reduced *sns1* expression remains impermeable to Eosin Y, and Sudan black detection of lipophilic components in the integument is positive. Attenuated dye penetration in *sns1* deficient larvae may be due to presence of these Sudan black-sensitive lipophilic molecules on their surface and their absence on the surface of *snu* deficient larvae. Dispensability of Sns1 in the wing suggests tissue-specific adjustment of Snu and Sns1 function. In any case, similarly to the *snu* mutant phenotype, based on ultrastructural analyses and by fluorescence microscopy, the envelope of larvae with reduced or eliminated Sns1 function appears to be aberrant or depleted. Based on the localisation of the Sns1 protein at the tips of the putative pore canals, we conclude that it indirectly participates in the construction of the envelope as an impermeability barrier. Moreover, the similar phenotype of larvae with reduced or eliminated *snu* and *sns1* function suggests that the respective proteins act in the same mechanism of envelope formation and function.

4.3. *Snu* and *Sns1* function is independent of the heme-biosynthesis pathway

Recently, we discovered that the heme-biosynthesis pathway is needed for water retention by the *Drosophila* larval cuticle (Shaik et al., 2012). A dityrosine network produced by a yet unknown heme-dependent peroxidase probably within the procuticle is reduced in these animals. Their envelope is, by contrast, normal and impermeable. Thus, the barrier formed in dependence of the heme biosynthesis pathway and the one formed by the presumed Snu-Sns1 pathway are separate

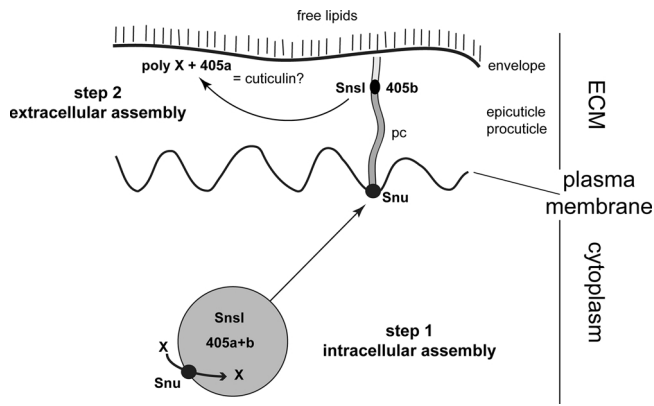


Fig. 9. Model for Snu and Sns1 function.

Snu localises to vesicles and is probably needed to load cuticle material (X) into these vesicles that also contain Sns1 and 405-dot precursors (405a + b). In these vesicles, a first step of inward barrier assembly may occur. They eventually fuse with the apical plasma membrane, and their content is released into the differentiating cuticle. Possibly via the putative pore canals, Sns1 and a subfraction of the 405-dot precursors (405a) are delivered to the distal regions of these canals. Another subfraction of 405-dot precursors (405b) and probably the Snu substrate X are used to form the envelope. The distribution of this subfraction of 405-dot depends also on Sns1 function. This second step of assembly in the extracellular space establishes the inward barrier of the cuticle.

structures. The Snu-Sns1-dependent envelope-borne barrier does not involve a di-tyrosine network.

4.4. Snu and Sns1 cooperate during envelope construction

How may Snu and Sns1 act together in envelope construction and function (Fig. 9)? Snu is an ABC transporter, an enzyme with multiple transmembrane domains, that predominantly localises to the apical plasma membrane of epidermal and tracheal cells during cuticle formation. It is required for correct localisation of the 405-dots and the extracellular protein Sns1-RFP in the mature cuticle. Besides, Snu is also detected in intracellular particles, which consistent with the transmembrane domains of Snu possibly constitute transport vesicles. Most Snu-positive putative vesicles also contain Sns1-RFP and the 405-dot material. It is well possible that a partner of the half-type ABC transporter Snu, i.e. another half-type ABC transporter is also associated with these structures. We suppose that these putative transport vesicles represent the site of the first step of envelope assembly within the cytoplasm. Of course, we cannot exclude that the intracellular signal pinpoints over-expression artefacts. In *snu* deficient animals, Sns1-RFP and the 405-dots largely co-localise in these putative vesicles suggesting that loading or formation of these structures with 405-dot material and Sns1-RFP is independent of Snu function. By contrast, Sns1-RFP and the 405-dots are mislocalised in the cuticle of *snu* deficient larvae. This finding indicates that the content of the 405-dot and Sns1-RFP vesicle-like compartments is not functional in the absence of Snu. Hence, in summary, Snu mediates loading of these putative vesicles with a substance that is needed for the successful localisation of the 405-dots and Sns1-RFP in the extracellular space after secretion. Conceivably, our lipid staining experiments with Sudan black argue that these components are lipophilic. This material, is present in *sns1* deficient (with normal Snu activity), but not in *snu* deficient larvae. In conclusion, the 405-dots, Sns1-RFP and the substrate of Snu together constitute an essential element of the envelope and of the sub-envelope region as a waterproof barrier.

This scenario implies that localisation of Snu in the apical plasma membrane is the consequence of vesicle fusion with the plasma membrane and that it has no significance for Snu function per se. In an alternative scenario, Snu may play an important role in the apical plasma membrane. Following this line of argument, Snu may be involved in the formation of the membranous putative pore canals that

are important routes of material transport to the cuticle surface including the envelope. Mislocalisation of Sns1-RFP and the 405-dots in *snu* deficient larvae would be a consequence of defective or inexistent putative pore canals. These alternative scenarios are shown in Fig. 9.

4.5. Parallels to vertebrate lipid-based ECM formation

In vertebrates, the extracellular pulmonary surfactant that stabilises alveolar structure during breathing is produced by ABCA3 that localises to alveolar type 2 epithelial cells (Beers and Mulugeta, 2017). Precursors of the surfactant are assembled first in ABCA3-harboured lamellar bodies that derive from multi-vesicular bodies. These vesicles are transported to the apical plasma membrane and their contents are released into the extracellular space. ABCA3 is eventually recycled back to lamellar bodies or degraded by lysosomes. Likewise, in keratinocytes, ABCA12 is essential for the formation of the lamellar bodies inside the cell before deposition into the extracellular space by a yet unknown mechanism (Feingold and Elias, 2014).

In *D. melanogaster*, a portion of Snu localises to putative intracellular vesicles that contain envelope precursors including lipids and Sns1, in addition, some other portion of Snu localises to the apical plasma membrane, while some Snu-positive putative vesicles within the cell, probably recycling endosomes, are devoid of Sns1 and/or envelope precursors.

In general, thus, production of lipid-based extracellular matrices may by default involve the activity of an ABC transporter that is needed to assemble minimal matrix units within putative intracellular vesicles. Based on our previous work on the function of the t-SNARE Syntaxin-1A (Syx1A) showing a depleted envelope in *syx1A* mutant larvae (Moussian et al., 2007), we reckon that subsequent release of the ECM units to the extracellular space may indeed depend on Syx1A. This mechanism is elusive in vertebrates.

4.6. Does the assembly of Wigglesworth's cuticulin depend on Snu?

Cuticulin is the key component of the envelope as a waterproof barrier (Wigglesworth, 1970, 1975). It is a complex composed of "wax and sclerotin" (Wigglesworth, 1985a), which itself is a protein-quinone complex of unknown composition. To what extent are our findings conform to the classical cuticulin concept of Wigglesworth?

Several aspects of Wigglesworth's cuticulin function are compromised in larvae with reduced or eliminated *snu* or *sns1* expression. Most importantly, the envelope of these animals is depleted and is unable to control inward and outward flow of water or xenobiotics (Eosin Y). Additionally, their head skeleton and denticles fail to melanise normally. Conceptually, following Wigglesworth's arguments, cuticulin assembly or function appears to be disrupted in these animals. Both proteins, however, do not localise to the envelope, but to a sub-envelope region (Sns1) or the apical plasma membrane (Snu). These data, hence, suggest together that Snu and Sns1 are not constituents of the envelope or cuticulin itself but mediate envelope construction possibly by assisting cuticulin assembly. The sub-envelope putative pore canal population of cuticulin i.e. 405-dots, on the contrary, do harbour Sns1 that may play a role in sealing these membranes.

A core component of cuticulin may be represented by the 405-material in the envelope and the 405-dots below the envelope. The 405-dots may be distinct structures or merely the storage or transport form of the 405-material. The absence of Sns1 in the envelope and depletion of the envelope in *sns1* mutant larvae argue together that the 405-dots are transported to the envelope in an Sns1-dependent mechanism, a process that starts already within the cell. For a full comprehension of the relationship between cuticulin and the 405-material, Snu and Sns1 the molecular composition of the 405-material needs to be identified and characterised.

Conflict of interest

The authors declare no conflict of interests.

Author contributions

Conceived and designed the experiments: MN, RZ and BM. Performed the experiments: MN, RZ, YW, KO, JB, NG, DA, MF and BM. Analyzed the data: MN, RZ, DA and BM. Wrote the paper: RZ, MN and BM.

Acknowledgments

We thank FlyBase and the Bloomington Drosophila Stock Center, for information and fly stocks. This work was supported by the DFG (grant number MO1714/6).

Appendix A. Supplementary data

Supplementary data associated with this article can be found, in the online version, at <https://doi.org/10.1016/j.ejcb.2017.12.003>.

References

- Beers, M.F., Mulugeta, S., 2017. The biology of the ABCA3 lipid transporter in lung health and disease. *Cell Tissue Res.* 367, 481–493.
- Broehan, G., Kroeger, T., Lorenzen, M., Merzendorfer, H., 2013. Functional analysis of the ATP-binding cassette (ABC) transporter gene family of *Tribolium castaneum*. *BMC Genomics* 14, 6.
- Chino, H., Katase, H., Downer, R.G., Takahashi, K., 1981. Diacylglycerol-carrying lipoprotein of hemolymph of the American cockroach: purification, characterization, and function. *J. Lipid Res.* 22, 7–15.
- Dietzl, G., Chen, D., Schnorrrer, F., Su, K.C., Barinova, Y., Fellner, M., Gasser, B., Kinsey, K., Oettel, S., Scheiblauer, S., Couto, A., Marra, V., Keleman, K., Dickson, B.J., 2007. A genome-wide transgenic RNAi library for conditional gene inactivation in *Drosophila*. *Nature* 448, 151–156.
- Feingold, K.R., Elias, P.M., 2014. Role of lipids in the formation and maintenance of the cutaneous permeability barrier. *Biochim. Biophys. Acta* 1841, 280–294.
- Fristrom, D., Liebrich, W., 1986. The hormonal coordination of cuticulin deposition and morphogenesis in *Drosophila* imaginal discs in vivo and in vitro. *Dev. Biol.* 114, 1–11.
- Gibbs, A., 1998. Water-Proofing properties of cuticular lipids. *Amer. Zool.* 38, 471–482.
- Gibbs, A.G., 2002. Lipid melting and cuticular permeability: new insights into an old problem. *J. Insect Physiol.* 48, 391–400.
- Gibbs, A.G., 2011. Thermodynamics of cuticular transpiration. *J. Insect Physiol.* 57, 1066–1069.
- Goerke, J., 1998. Pulmonary surfactant: functions and molecular composition. *Biochim. Biophys. Acta* 1408, 79–89.
- Graveley, B.R., Brooks, A.N., Carlson, J.W., Duff, M.O., Landolin, J.M., Yang, L., Artieri, C.G., van Baren, M.J., Boley, N., Booth, B.W., Brown, J.B., Chervas, L., Davis, C.A., Dobin, A., Li, R., Lin, W., Malone, J.H., Mattiuzzo, N.R., Miller, D., Sturgill, D., Tusch, B.B., Zaleski, C., Zhang, D., Blanchette, M., Dudoit, S., Eads, B., Green, R.E., Hammonds, A., Jiang, L., Kapranov, P., Langton, L., Perrimon, N., Sandler, J.E., Wan, K.H., Willingham, A., Zhang, Y., Zou, Y., Andrews, J., Bickel, P.J., Brenner, S.E., Brent, M.R., Chervas, P., Gingeras, T.R., Hoskins, R.A., Kaufman, T.C., Oliver, B., Celniker, S.E., 2011. The developmental transcriptome of *Drosophila melanogaster*. *Nature* 471, 473–479.
- Hartenstein, V., Campos-Ortega, J.A., 1985. The embryonic development of *Drosophila melanogaster*. Springer-Verlag, Berlin; New York.
- Koster, M.I., 2009. Making an epidermis. *Ann. N. Y. Acad. Sci.* 1170, 7–10.
- Kumar, S., Konikoff, C., Van Emden, B., Busick, C., Davis, K.T., Ji, S., Wu, L.W., Ramos, H., Brody, T., Panchanathan, S., Ye, J., Karr, T.L., Gerold, K., McCutchan, M., Newfield, S.J., 2011. FlyExpress: visual mining of spatiotemporal patterns for genes and publications in *Drosophila* embryogenesis. *Bioinformatics* 27, 3319–3320.
- Locke, M., 1961. Pore canals and related structures in insect cuticle. *J. Biophys. Biochem. Cytol.* 10, 589–618.
- Moussian, B., Schwarz, H., 2010. Preservation of plasma membrane ultrastructure in *Drosophila* embryos and larvae prepared by high-pressure freezing and freeze-substitution. *Drosophila Inf. Serv.* 93, 215–219.
- Moussian, B., Schwarz, H., Bartoszewski, S., Nusslein-Volhard, C., 2005. Involvement of chitin in exoskeleton morphogenesis in *Drosophila melanogaster*. *J. Morphol.* 264, 117–130.
- Moussian, B., Seifarth, C., Muller, U., Berger, J., Schwarz, H., 2006a. Cuticle differentiation during *Drosophila* embryogenesis. *Arthropod Struct. Dev.* 35, 137–152.
- Moussian, B., Tang, E., Tønning, A., Helms, S., Schwarz, H., Nusslein-Volhard, C., Uv, A.E., 2006b. *Drosophila* Knickkopf and Retroactive are needed for epithelial tube growth and cuticle differentiation through their specific requirement for chitin filament organization. *Development* 133, 163–171.
- Moussian, B., Veerkamp, J., Muller, U., Schwarz, H., 2007. Assembly of the *Drosophila* larval exoskeleton requires controlled secretion and shaping of the apical plasma membrane. *Matrix Biol.* 26, 337–347.
- Moussian, B., 2010. Recent advances in understanding mechanisms of insect cuticle differentiation. *Insect Biochem. Mol. Biol.* 40, 363–375.
- Nüsslein-Volhard, C., Wieschaus, E., Kluding, H., 1984. Mutations affecting the pattern of the larval cuticle in *Drosophila melanogaster*: i. Zygotic loci on the second chromosome. *Roux's Arch. Dev. Biol.* 193, 267–282.
- Nishifuji, K., Yoon, J.S., 2013. The stratum corneum: the rampart of the mammalian body. *Vet. Dermatol.* 24, 60–72 (e15–66).
- Palm, W., Sampaio, J.L., Brankatschk, M., Carvalho, M., Mahmoud, A., Shevchenko, A., Eaton, S., 2012. Lipoproteins in *Drosophila melanogaster*? assembly, function, and influence on tissue lipid composition. *PLoS Genet.* 8, e1002828.
- Roberson, E.D., Bowcock, A.M., 2010. Psoriasis genetics: breaking the barrier. *Trends Genet.* 26, 415–423.
- Shaik, K.S., Meyer, F., Vazquez, A.V., Flotenmeyer, M., Cerdan, M.E., Moussian, B., 2012. delta-Aminolevulinic synthase is required for apical transcellular barrier formation in the skin of the *Drosophila* larva. *Eur. J. Cell Biol.* 91, 204–215.
- Wang, Y., Zuber, R., Oehl, K., Norum, M., Moussian, B., 2015. Report on *Drosophila melanogaster* larvae without functional tracheae. *J. Zool.* 296, 139–145.
- Wang, Y., Yu, Z., Zhang, J., Moussian, B., 2016. Regionalization of surface lipids in insects. *Proc. Biol. Sci.* 283.
- Wang, Y., Carballo, R.G., Moussian, B., 2017. Double cuticle barrier in two global pests, the whitefly *Trialeurodes vaporariorum* and the bedbug *Cimex lectularius*. *J. Exp. Biol.*
- Wigglesworth, V.B., 1933. The physiology of the cuticle and of ecdysis in *Rhodnius prolixus* (Triatomidae: hemiptera); with special reference to the oenocytes and function of the dermal glands. *Quart. J. Microscop. Soc.* 76, 270–318.
- Wigglesworth, V.B., 1946. The epicuticle of an insect, *Rhodnius prolixus* (Hemiptera). *Proc. R. Soc. Lond. B Biol. Sci.* 134, 163–181.
- Wigglesworth, V.B., 1970. Structural lipids in the insect cuticle and the function of the oenocytes. *Tissue Cell* 2, 155–179.
- Wigglesworth, V.B., 1975. Distribution of lipid in the lamellate endocuticle of *Rhodnius prolixus* (Hemiptera). *J. Cell Sci.* 19, 439–457.
- Wigglesworth, V.B., 1985a. Sclerotin and lipid in the waterproofing of the insect cuticle. *Tissue Cell* 17, 227–248.
- Wigglesworth, V.B., 1985b. The transfer of lipid in insects from the epidermal cells to the cuticle. *Tissue Cell* 17, 249–265.
- Wigglesworth, V.B., 1988. The source of lipids and polyphenols for the insect cuticle: the role of fat body, oenocytes and oenocytoids. *Tissue Cell* 20, 919–932.
- Wigglesworth, V.B., 1990. The distribution, function and nature of cuticulin in the insect cuticle. *J. Insect Physiol.* 36, 307–313.
- Yu, Z., Wang, Y., Zhao, X., Liu, X., Ma, E., Moussian, B., Zhang, J., 2017. The ABC transporter ABCH-9C is needed for cuticle barrier construction in *Locusta migratoria*. *Insect Biochem. Mol. Biol.* 87, 90–99.
- Zhang, S., Feany, M.B., Saraswati, S., Littleton, J.T., Perrimon, N., 2009. Inactivation of *Drosophila* Huntingtin affects long-term adult functioning and the pathogenesis of a Huntington's disease model. *Dis. Model Mech.* 2, 247–266.
- van Smeden, J., Janssens, M., Gooris, G.S., Bouwstra, J.A., 2014. The important role of stratum corneum lipids for the cutaneous barrier function. *Biochim. Biophys. Acta* 1841, 295–313.

Acknowledgement - Danksagung

Als erstes möchte ich PD Dr. Bernard Moussian, Professor Dr. Matthias Schwab und Professor Dr. Anne Nies für die wertvollen Diskussionen im Verlauf der Promotion, ihre lektorische Unterstützung, sowie persönlichen, wie wissenschaftlichen Rat danken.

Danken möchte ich auch meiner Labor-Kollegin Nicole Gehring für ihre Hilfe in dem Alltag im Labor.

Zum Schluss danke ich meinen Eltern und meiner Familie für ihre Unterstützung während meiner Schulzeit, meines Studiums und der Promotion. Eure Hilfe bot mir immer großen Rückhalt.

CURRICULUM VITAE

Personal Information

Family name: Wang
First name: Yiwen
Nationality: China
Date of Birth: April 11th 1984
Place of Birth: Tianjin

Education

College Education

2002-2006 Studied Software Engineering in Jilin University, China;
2003-2006 Studied Biotechnology in Jilin University
July 2006 Awarded the degree of B.S. of Soft Engineering
Awarded the second degree of B.S. of Biotechnology
2008-2011 Studied Biology at the Eberhard Karls University of Tübingen
August 2011 Awarded the degree of B.S. of Biology
with an average mark of 1.8 (Good)

2011-2014 Studied Master Course of Biology in Eberhard Karls University of
Tübingen. Awarded the degree of M.S. of Biology with an average
mark 1.3 (Very Good)

Since 2014 Ph.D student in Eberhard Karls University of Tübingen, IFIZ Animal
Genetic. Ph.D.

School

1999-2002 Nankai-Xiangyu High School Tianjin
1996-1999 Nanying Middle School Tianjin

1990-1996 Primary School of Tianjin University

Languages

English: communicational

CET 4 of College English Test (China)

German: fluent

DSH 2

Portuguese: basic

Publication List

First author

2014

Wang, Yiwen; Odemer, Richard; Rosenkranz, Peter; Moussian, Bernard (2014): **Putative orthologues of genetically identified *Drosophila melanogaster* chitin producing and organising genes in *Apis mellifera***. *Apidologie* (2014) 45: 733. doi:10.1007/s13592-014-0292-3

2015

Wang, Yiwen.; Zuber, Renata.; Oehl, Kathrin.; Norum, Micheala.; Moussian, Bernard. (2015): **Report on *Drosophila melanogaster* larvae without functional tracheae**. In: *J Zool* 296 (2), S. 139–145. DOI: 10.1111/jzo.12226.

Wang, Yiwen; Cruz, Tina; Irion, Uwe; Moussian, Bernard (2015): **Differentiated muscles are mandatory for gas-filling of the *Drosophila* airway system**. In: *Biology open* 4 (12), S. 1753–1761. DOI: 10.1242/bio.013086.

2016

Wang, Yiwen; Yu, Zhitao; Zhang, Jianzhen; Moussian, Bernard (2016): **Regionalization of surface lipids in insects**. In: *Proceedings. Biological sciences* 283 (1830). DOI: 10.1098/rspb.2015.2994.

Wang, Yiwen; da Cruz, Tina Correia; Pulfemuller, Alicia; Gregoire, Stephane; Ferveur, Jean-Francois; Moussian, Bernard (2016): **INHIBITION OF FATTY ACID DESATURASES IN *Drosophila melanogaster* LARVAE BLOCKS**

FEEDING AND DEVELOPMENTAL PROGRESSION. In: *Archives of insect biochemistry and physiology* 92 (1), S. 6–23. DOI: 10.1002/arch.21329.

2017

Wang, Yiwen; Zuber, Renata; Laudahn, Annette; Berger, Jurgen; Moussian, Bernard (2017): **Cuticular body hairs mediate clumping of small *Camponotus floridanus* larvae.** In: *Arthropod structure & development* 46 (1), S. 108–115. DOI: 10.1016/j.asd.2016.12.003.

Wang, Yiwen; Carballo, Rocio Gallego; Moussian, Bernard (2017): **Double cuticle barrier in two global pests, the whitefly *Trialeurodes vaporariorum* and the bedbug *Cimex lectularius*.** In: *The Journal of experimental biology* 220 (Pt 8), S. 1396–1399. DOI: 10.1242/jeb.156679.

2018

Wang, Yiwen; Berger, Jürgen; Moussian, Bernard (2018): **Trynity models a tube valve in the *Drosophila* larval airway system.** In: *Developmental Biology* 437 (2), S. 75– 83. DOI: 10.1016/j.ydbio. 2018.02.019

Wang, Yiwen; Moussian, Bernard; Schaeffeler, Elke; Schwab Matthias; Nies, Anne T. (2018): **The fruit fly *Drosophila melanogaster* as an innovative preclinical ADME model for solute carrier membrane transporters with consequences for pharmacology and drug therapy.** In: *Drug Discovery Today*. Accepted.

Co-author

Shaik, Khaleelulla Saheb; Wang, Yiwen; Aravind, L.; Moussian, Bernard (2014): **The Knickkopf DOMON domain is essential for cuticle differentiation in *Drosophila melanogaster*.** In: *Archives of insect biochemistry and physiology* 86 (2), S. 100–106. DOI: 10.1002/arch.21165.

Yu, Zhitao; Zhang, Xueyao; Wang, Yiwen; Moussian, Bernard; Zhu, Kun Yan; Li, Sheng et al. (2016): **LmCYP4G102: An oenocyte-specific cytochrome P450 gene required for cuticular waterproofing in the migratory locust, *Locusta migratoria*.** In: *Scientific reports* 6, S. 29980. DOI: 10.1038/srep29980.

Yu, Zhitao; Wang, Yiwen; Zhao, Xiaoming; Liu, Xiaojian; Ma, Enbo; Moussian, Bernard; Zhang, Jianzhen (2017): **The ABC transporter ABCH-9C is needed for cuticle barrier construction in *Locusta migratoria*.** In: *Insect biochemistry and molecular biology* 87, S. 90–99. DOI: 10.1016/j.ibmb.2017.06.005.

Zuber, Renata; Norum, Michaela; Wang, Yiwen; Oehl, Kathrin; Gehring, Nicole; Accardi, Davide; Bartozsewski, Slawomir; Berger, Jürgen; Flotenmeyer, Matthias and Moussian, Bernard (2018). **The ABC transporter Snu and the**

extracellular protein Sns1 cooperate in the formation of the lipid-based inward and outward barrier in the skin of *Drosophila*. In: Eur J Cell Biol. 97(2), S. 90-101. DOI: 10.1016/j.ejcb.2017.12.003.

Disclosures-Erklärungen:

Hiermit erkläre ich nach §5(2) der Promotionsordnung der Mathematisch-Naturwissenschaftlichen Fakultät der Universität Tübingen, dass:

- dies mein erstes Promotionsverfahren ist (§ 5.2.4)
- ich die vorliegende Dissertation selbstständig und unter ausschließlicher Verwendung der angegebenen Quellen und Hilfsmittel angefertigt und wörtlich oder inhaltlich übernommene Stellen als solche gekennzeichnet habe. Beiträge anderer Personen zu dieser Arbeit wurden an entsprechender Stelle gekennzeichnet (§ 5.2.6)
- mir das Promotionsverfahren nicht kommerziell vermittelt wurde (§ 5.2.8)
- keine Personen oder Organisationen beteiligt waren, die gegen Entgelt Betreuer vermitteln oder mich meiner mir obliegenden Pflichten bezüglich der Prüfungsleistungen ganz oder teilweise entledigen (§ 5.2.8)
- keine strafrechtlichen Verurteilungen, Disziplinarmaßnahmen und abhängige Straf- und Disziplinarverfahren zu meiner Person vorliegen (§ 5.2.9)